5. Li LH, Fraser TJ, Olin EJ, Bhuyan BK. Action of camptothecin on mammalian cells in culture. Cancer Res 1972;32:2643–50.
6. Gallo RC, Whang-Peng J, Adamson RH. Studies on the antitumor activity, mechanism of action, and cell cycle effects of camptothecin. J Natl Cancer Inst 1971;46:789–95.
7. Friedman HS, Petros WP, Friedman AH, Schaaf LJ, Kerby T, Lawyer J, Parry M, Houghton PJ, Lovell S, Rasheed K, Cloughsey T, Stewart ES, et al. Irinotecan therapy in adults with recurrent or progressive malignant glioma. J Clin Oncol 1999;17:1516–25.
8. Cloughesy TF, Filka E, Kuhn J, Nelson G, Kabbinavar F, Friedman H, Miller LL, Elfring GL. Two studies evaluating irinotecan treatment for recurrent malignant glioma using an every-3-week regimen. Cancer 2003;97:2381–6.
9. Chamberlain MC. Salvage chemotherapy with CPT-11 for recurrent glioblastoma multiforme. J Neurooncol 2002;56:183–8.
10. Prados MD, Lamborn K, Yung WK, Jaeckle K, Robins HI, Mehta M, Fine HA, Wen PY, Cloughesy T, Chang S, Nicholas MK, Schiff D, et al. A phase 2 trial of irinotecan (CPT-11) in patients with recurrent malignant glioma: a North American brain tumor consortium study. Neuro Oncol 2006;8:189–93.
11. Vredenburgh JJ, Desjardins A, Herndon JE, II, Dowell JM, Reardon DA, Quinn JA, Rich JN, Sathornsumetee S, Gururangan S, Wagner M, Bigner DD, Friedman AH, et al. Phase II trial of bevacizumab and irinotecan in recurrent malignant glioma. Clin Cancer Res 2007;13:1253–9.
12. Vredenburgh JJ, Desjardins A, Herndon JE, II, Marcello J, Reardon DA, Quinn JA, Rich JN, Sathornsumetee S, Gururangan S, Sampson J, Wagner M, Bailey L, et al. Bevacizumab plus irinotecan in recurrent glioblastoma multiforme. J Clin Oncol 2007;25:4722–9.
13. Gradishar WJ. Albumin-bound nanoparticle paclitaxel. Clin Adv Hematol Oncol 2005;3:348–9.
14. Muggia FM. Liposomal encapsulated anthracyclines: new therapeutic horizons. Curr Oncol Rep 2001;3:156–62.
15. Slatter JG, Schaaf LJ, Sams JP, Feenstra KL, Johnson MG, Bombardt PA, Cathcart KS, Verburg MT, Pearson LK, Compton LD, Miller LL, Baker DS, et al. Pharmacokinetics, metabolism, and excretion of irinotecan (CPT-11) following I.V. infusion of [(14)C]CPT-11 in cancer patients. Drug Metab Dispos 2000;28:423–33.
16. Rothenberg ML, Kuhn JG, Burris HA, III, Nelson J, Eckardt JR, Tristan-Morales M, Hilsenbeck SG, Weiss GR, Smith LS, Rodriguez GI, et al. Phase I and pharmacokinetic trial of weekly CPT-11. J Clin Oncol 1993;11:2194–204.
17. Koizumi F, Kitagawa M, Negishi T, Onda T, Matsumoto S, Hamaguchi T, Matsumura Y. Novel SN-38-incorporating polymeric micelles, NK012, eradicate vascular endothelial growth factor-secreting bulky tumors. Cancer Res 2006;66:10048–56.
18. Sumitomo M, Koizumi F, Asano T, Horiguchi A, Ito K, Kakizoe T, Hayakawa M, Matsumura Y. Novel SN-38-incorporated polymeric micelle, NK012, strongly suppresses renal cancer progression. Cancer Res 2008;68:1631–5.
19. Nakajima TE, Yasunaga M, Kano Y, Koizumi F, Kato K, Hamaguchi T, Yamada Y, Shirao K, Shimada Y, Matsumura Y. Synergistic antitumor activity of the novel SN-38-incorporating polymeric micelles, NK012, combined with 5-fluorouracil in a mouse model of colorectal cancer, as compared with that of irinotecan plus 5-fluorouracil. Int J Cancer 2008;122:2148–53.
20. Saito Y, Yasunaga M, Kuroda J, Koga Y, Matsumura Y. Enhanced distribution of NK012, a polymeric micelle-encapsulated SN-38, and sustained release of SN-38 within tumors can beat a hypovascular tumor. Cancer Sci 2008;99:1258–64.
21. Kawato Y, Furuta T, Aonuma M, Yasuoka M, Yokokura T, Matsumoto K. Antitumor activity of a camptothecin derivative, CPT-11, against human tumor xenografts in nude mice. Cancer Chemother Pharmacol 1991;28:192–8.
22. Matsumura Y, Maeda H. A new concept for macromolecular therapeutics in cancer chemotherapy: mechanism of tumoritropic accumulation of proteins and the antitumor agent smancs. Cancer Res 1986; 46:6387–92.
23. Maeda H, Matsumura Y, Kato H. Purification and identification of [hydroxyprolyl3]bradykinin in ascitic fluid from a patient with gastric cancer. J Biol Chem 1988;263:16051–4.
24. Matsumura Y, Maruo K, Kimura M, Yamamoto T, Konno T, Maeda H. Kinin-generating cascade in advanced cancer patients and in vitro study. Jpn J Cancer Res 1991;82:732–41.
25. Dvorak HF, Nagy JA, Dvorak JT, Dvorak AM. Identification and characterization of the blood vessels of solid tumors that are leaky to circulating macromolecules. Am J Pathol 1988;133:95–109.
26. Leung DW, Cachianes G, Kuang WJ, Goeddel DV, Ferrara N. Vascular endothelial growth factor is a secreted angiogenic mitogen. Science 1989;246:1306–9.
27. Abe K, Shoji M, Chen J, Bierhaus A, Danave I, Micko C, Casper K, Dillehay DL, Nawroth PP, Rickles FR. Regulation of vascular endothelial growth factor production and angiogenesis by the cytoplasmic tail of tissue factor. Proc Natl Acad Sci USA 1999;96:8663–8.
28. Belting M, Dorrell MI, Sandgren S, Aguilar E, Ahamed J, Dorfleutner A, Carmeliet P, Mueller BM, Friedlander M, Ruf W. Regulation of angiogenesis by tissue factor cytoplasmic domain signaling. Nat Med 2004;10:502–9.
29. Rong Y, Post DE, Pieper RO, Durden DL, Van Meir EG, Brat DJ. PTEN and hypoxia regulate tissue factor expression and plasma coagulation by glioblastoma. Cancer Res 2005;65:1406–13.
30. Hamada K, Kuratsu J, Saitoh Y, Takeshima H, Nishi T, Ushio Y. Expression of tissue factor correlates with grade of malignancy in human glioma. Cancer 1996;77:1877–83.
31. Takano S, Yoshii Y, Kondo S, Suzuki H, Maruno T, Shirai S, Nose T. Concentration of vascular endothelial growth factor in the serum and tumor tissue of brain tumor patients. Cancer Res 1996;56:2185–90.
32. Chowdhary S, Wong ET. Bevacizumab combined with irinotecan for recurrent glioblastoma multiforme–improvement over available therapy? Nat Clin Pract Neurol 2008;4:242–3.
33. Chamberlain MC Bevacizumab plus irinotecan in recurrent glioblastoma. J Clin Oncol 2008;26:1012–3.
34. Plate KH, Breier G, Weich HA, Risau W. Vascular endothelial growth factor is a potential tumour angiogenesis factor in human gliomas in vivo. Nature 1992;359:845–8.
35. Horten BC, Basler GA, Shapiro WR. Xenograft of human malignant glial tumors into brains of nude mice. A histopatholgical study. J Neuropathol Exp Neurol 1981;40:493–511.
36. Giannini C, Sarkaria JN, Saito A, Uhm JH, Galanis E, Carlson BL, Schroeder MA, James CD. Patient tumor EGFR and PDGFRA gene amplifications retained in an invasive intracranial xenograft model of glioblastoma multiforme. Neuro Oncol 2005;7:164–76.
37. Engebraaten O, Hjortland GO, Hirschberg H, Fodstad O. Growth of precultured human glioma specimens in nude rat brain. J Neurosurg 1999;90:125–32.
38. Galli R, Binda E, Orfanelli U, Cipelletti B, Gritti A, De Vitis S, Fiocco R, Foroni C, Dimeco F, Vescovi A. Isolation and characterization of tumorigenic, stem-like neural precursors from human glioblastoma. Cancer Res 2004;64:7011–21.
39. Gunther HS, Schmidt NO, Phillips HS, Kemming D, Kharbanda S, Soriano R, Modrusan Z, Meissner H, Westphal M, Lamszus K. Glioblastoma-derived stem cell-enriched cultures form distinct subgroups according to molecular and phenotypic criteria. Oncogene 2008;27:2897–909.
40. Onda T, Nakamura I, Seno C, Matsumoto S, Kitagawa M, Okamoto K, Nishikawa K, Suzuki M. Superior antitumor activity of NK012, 7-etyhl-10-hydroxycamptothecin-incorporating micellar nanoparticle, to irinotecan [abstruct 3062]. Proc Am Assoc Cancer Res 2006;47:720s.
41. Kato K, Hamaguchi T, Shirao K, Shimada Y, Doi T, Ohtsu A, Matsumura Y, Yamada Y. Interim analysis of phase I study of NK012, polymer micelle SN-38, in patients with advanced cancer. Proc Am Soc Clin Oncol GI 2008 (Abstract no 485).
42. Burris HA, III, Infante JR, Spigel DR, Greco FA, Thompson DS, Matsumoto S, Kawamura S, Jones SF. A phase I dose-escalation study of NK012. Proc Am Soc Clin Oncol 2008 (Abstract no 2538).

Antitumor Activity of NK012 Combined with Cisplatin against Small Cell Lung Cancer and Intestinal Mucosal Changes in Tumor-Bearing Mouse after Treatment

Tatsuya Nagano,[1,2,3] Masahiro Yasunaga,[1] Koichi Goto,[2] Hirotsugu Kenmotsu,[2] Yoshikatsu Koga,[1] Jun-ichiro Kuroda,[1] Yoshihiro Nishimura,[3] Takashi Sugino,[4] Yutaka Nishiwaki,[2] and Yasuhiro Matsumura[1]

Abstract

Purpose: To investigate the advantages of treatment with the SN-38–incorporating polymeric micelles NK012 over CPT-11 in combination with cisplatin [*cis*-dichlorodiammineplatinum (II) (CDDP)] in mice bearing a small cell lung cancer xenograft in terms of antitumor activity and toxicity, particularly intestinal toxicity.

Experimental Design: Cytotoxic effects were evaluated in human small cell lung cancer cell lines [H69, H82, and vascular endothelial growth factor (VEGF)–secreting cells (SBC-3/VEGF and its mock transfectant SBC-3/Neo)]. *In vivo* antitumor effects were evaluated in SBC-3/Neo–bearing and SBC-3/VEGF–bearing mice after NK012/CDDP or CPT-11/CDDP administration on days 0, 7, and 14. Drug distribution was analyzed by high-performance liquid chromatography or fluorescence microscopy, and the small intestine was pathologically examined.

Results: The *in vitro* growth-inhibitory effects of NK012 were 198- to 532-fold more potent than those of CPT-11. A significant difference in the relative tumor volume on day 30 was found between NK012/CDDP and CPT-11/CDDP treatments ($P = 0.0058$). Inflammatory changes in the small intestinal mucosa were rare in all NK012-treated mice but were commonly observed in CPT-11–treated mice. Moreover, a large amount of CPT-11 was excreted into the feces and high CPT-11 concentration was detected in the small intestinal epithelium. On the other hand, a small amount of NK012 was found in the feces and NK012 was weakly and uniformly distributed in the mucosal interstitium.

Conclusions: NK012/CDDP combination may be a promising candidate regimen against lung cancer without severe diarrhea toxicity and therefore warrants further clinical evaluation.

SN-38 or 7-ethyl-10-hydroxy-camptothecin is a biologically active metabolite of irinotecan hydrochloride (CPT-11) and is formed through CPT-11 conversion by carboxylesterases. SN-38 is active against various human cancers, such as colorectal, lung, and ovarian cancer (1–4). Although SN-38 shows up to 1,000-fold more potent cytotoxic activity against various cancer cell lines than CPT-11 *in vitro* (5), it has been clinically unavailable because of its water-insoluble nature, and the conversion rate from CPT-11 to SN-38 is <10% of the original CPT-11 volume in the body (6, 7).

The SN-38–incorporating polymeric micelles NK012 seem to have the advantage of passive targeting of the drug delivery system. In this passive targeting of drug delivery system, the drug accumulates in tumor tissue by using the enhanced permeability and retention effect (8–11). This enhanced permeability and retention effect is based on several pathologic mechanisms, which include hypervascularity, secretion of tumor vascular permeability factors stimulating extravasation of macromolecules including nanoparticles such as liposomes and micelles, and the absence of an effective lymphatic drainage of macromolecules accumulated in solid tumor tissue. Recent studies showed that NK012 has a significantly more potent antitumor activity than CPT-11 against small cell lung cancer (SCLC; ref. 12), colorectal cancer (13), renal cancer (14), pancreatic cancer (15), stomach cancer (16), and glioma (17).

It was previously reported that the SN-38/*cis*-dichlorodiammineplatinum (II) (CDDP) combination showed synergistic effects (18). The median survival of SCLC patients treated with the CPT-11/cisplatin (CDDP) combination was significantly longer than that of SCLC patients treated with the etoposide/CDDP combination in a randomized phase III study ($P = 0.002$) conducted by the Japanese Cooperative Oncology

Authors' Affiliations: [1]Investigative Treatment Division, Research Center for Innovative Oncology and [2]Thoracic Oncology Division, National Cancer Center Hospital East, Chiba, Japan; [3]Division of Respiratory Medicine, Department of Internal Medicine, Kobe University Graduate School of Medicine, Kobe, Japan; and [4]Department of Pathology, Fukushima Medical University School of Medicine, Fukushima, Japan

Received 12/25/08; revised 3/3/09; accepted 3/9/09; published OnlineFirst 6/9/9.

Grant support: Grant-in-Aid from the Third Term Comprehensive Control Research for Cancer; Ministry of Health, Labor and Welfare grant H19-025 (K. Goto, Y. Nishiwaki, and Y. Matsumura); Ministry of Education, Culture, Sports, Science and Technology Scientific Research on Priority Areas grant 17016087 (Y. Matsumura); and Japanese Foundation for Multidisciplinary Treatment of Cancer (Y. Matsumura), and the Princess Takamatsu Cancer Research Fund (07-23908).

The costs of publication of this article were defrayed in part by the payment of page charges. This article must therefore be hereby marked *advertisement* in accordance with 18 U.S.C. Section 1734 solely to indicate this fact.

Requests for reprints: Yasuhiro Matsumura, Investigative Treatment Division, Research Center for Innovative Oncology, National Cancer Center Hospital East, 6-5-1 Kashiwanoha, Kashiwa, Chiba 277-8577, Japan. Phone: 81-4-7133-1111, ext. 5400; Fax: 81-4-7134-6866; E-mail: yhmatsum@east.ncc.go.jp.

doi:10.1158/1078-0432.CCR-08-3334

Translational Relevance

The SN-38–incorporating polymeric micelles NK012 has been shown to have significant antitumor activity against several cancer mouse models compared with CPT-11. The phase I study showed that patients treated with NK012 did not develop grade 3/4 diarrhea, one of the major adverse effects of CPT-11. Here, the antitumor activity of NK012/cisplatin combination was compared with that of CPT-11/cisplatin combination, one of the most active regimens against SCLC and NSCLC in the clinic. We also evaluated the pharmacologic and toxic profiles of the drug combinations, particularly in terms of diarrhea. NK012/cisplatin showed a significant potent antitumor activity against an SBC-3 xenograft compared with CPT-11/cisplatin. Moreover, inflammatory pathologic changes were rarely observed in the small intestinal mucosa of the NK012-treated mouse but were commonly observed in the CPT-11–treated mouse. NK012/cisplatin combination chemotherapy is thus a promising regimen against lung cancer without severe diarrhea toxicity and therefore warrants further clinical evaluation.

Group (19). Therefore, CPT-11/CDDP is considered to be one of the most active regimens against SCLC in Japan. A recent randomized phase III study showed that CPT-11/CDDP was equal to other platinum-based regimens, such as carboplatin plus paclitaxel, CDDP plus gemcitabine, and CDDP plus vinorelbine, in terms of response rate and overall survival in non-SCLC (NSCLC) patients (20).

One of the major clinically important toxic effects or dose-limiting factors of CPT-11 is severe late-onset diarrhea (21–23). We previously showed that there was no significant difference in the kinetic character of free SN-38 in the small intestine of mice bearing the SCLC cell line SBC-3 and treated with NK012 and CPT-11 (12). Furthermore, in two independent phase I clinical trials in Japan (24) and the United States (25), nonhematologic toxicities were minimal and grade 3/4 diarrhea was absent.

In this context, we conducted this study to investigate the advantages of NK012/CDDP over CPT-11/CDDP in mice bearing a SCLC xenograft in terms of antitumor activity and toxic effects, particularly intestinal toxicity.

Materials and Methods

Drugs and cells. SN-38 and NK012 were prepared by Nippon Kayaku Co. Ltd. CPT-11 was purchased from Yakult Honsha Co. Ltd. CDDP was obtained from WC Heraeus GmbH & Co. KG.

Among the SCLC cell lines used, SBC-3 was kindly provided by Dr. I. Kimura (Okayama University, Okayama, Japan), and H69 and H82 were purchased from the American Type Culture Collection. SBC-3, H69, and H82 were maintained in RPMI 1640 supplemented with 10% fetal bovine serum (Cell Culture Technologies) and penicillin, streptomycin, and amphotericin B (100 units/mL, 100 μg/mL, and 25 μg/mL, respectively; Sigma) in a humidified atmosphere containing 5% CO_2 at 37°C. Vascular endothelial growth factor (VEGF)–secreting cells, SBC-3/VEGF and its mock transfectant SBC-3/Neo, were generated from SBC-3 cells transfected with BMG-Neo-VEGF and BMG-Neo, as described (26).

In vitro study. The growth-inhibitory effects of NK012, CPT-11, SN-38, and CDDP were examined by tetrazolium salt–based proliferation assay (WST-8 assay; Wako Chemicals). One hundred microliters of a suspension of exponentially growing cells (1×10^5/mL of SBC-3/Neo and SBC-3/VEGF or 1×10^6/mL of H69 and H82) were placed into the wells of a 96-well plate and incubated for 24 h at 37°C. Then, after medium removal, 100 μL of medium containing various concentrations of each drug were added to the wells and then incubated for 72 h at 37°C. After medium removal, 10 μL of WST-8 solution and 90 μL of medium were added to the wells followed by incubation for 1 h at 37°C. The growth-inhibitory effects of each drug were assessed spectrophotometrically (SpectraMax 190, Molecular Devices Corp.). The IC_{50} value was determined on the dose-response curves. The nature of interaction between NK012 and CDDP against SCLC cell lines, SBC-3/Neo, SBC-3/VEGF, H69, and H82, was evaluated by median-effect plot analyses and the combination index method of Chou and Talalay (27).

Experimental mice model. Female BALB/c nude mice (6 wk old) were purchased from SLC Japan. Mice were inoculated s.c. in the flank with 1×10^7 cells/150 μL cell suspension of SBC-3/Neo and SBC-3/VEGF cell lines.

All animal procedures were done in compliance with the guidelines for the care and use of experimental animals established by the Committee for Animal Experimentation of the National Cancer Center; these guidelines meet the ethical standards required by law and also comply with the guidelines for the use of experimental animals in Japan.

In vivo growth inhibition assay. When the tumor volume (TV) reached 1,500 mm^3, mice were randomly divided into test groups consisting of five mice per group (day 0). Drugs were i.v. administered into the tail vein on days 0, 7, and 14. NK012 was given at SN-38 equivalent doses of 10 and 5 mg/kg/d, which are one third and one sixth of the maximum tolerated dose, respectively. The reference drug, CPT-11, was given at 22 and 10 mg/kg/d, which are one third and one sixth of the maximum tolerated dose, respectively. CDDP was simultaneously given on the same day at 2.5 mg/kg/d based on a previous report (28). In preliminary experiment, NK012 (5 mg/kg) plus CDDP (2.5 mg/kg) seemed to be superior to NK012 (5 mg/kg) alone in these tumors. NaCl solution (0.9%) was administered i.v. as normal control. The length (a) and width (b) of the tumor masses and body weight (BW) were measured twice a week, and TV was calculated using $TV = (a \times b^2) / 2$. Relative TV (RTV) on day n was calculated using $RTV = TV_n / TV_0$, where TV_n is the TV on day n and TV_0 is the TV on day 0. Relative BW (RBW) was calculated using $RBW = BW_n / BW_0$. Differences in RTV and RBW between the treatment groups on day 30 were analyzed using the unpaired t test.

Pharmacokinetic analysis by high-performance liquid chromatography. Female BALB/c nude mice ($n = 3$) bearing SBC-3/Neo and SBC-3/VEGF tumors (1,500 mm^3) were used for drug pharmacokinetic analysis. NK012 or CPT-11 was administered at an equimolar dose of 20 or 30 mg/kg on day 0, respectively, as reported (12). CDDP was simultaneously given at 2.5 mg/kg. Mice were sacrificed 1, 6, 24, and 72 h (day 3) after administration. Plasma samples, tumors, upper small intestine, and feces were obtained and stored at -80°C until analysis.

SN-38 was extracted for each sample and reversed-phase high-performance liquid chromatography was done as reported (12).

Pathologic studies of small intestinal mucosa. CPT-11 and NK012 were injected to female BALB/c nude mice ($n = 3$) at the same dose schedules as those used in the treatment experiment. On day 14 after the last dosing, mice were sacrificed and parts of the small intestine were sampled at 5 cm from the pylolic part for the jejunum and 5 cm from the ileocecal junction for the ileum. Samples were fixed in 10% formalin, paraffin embedded, sectioned, and stained with H&E. Inflammation was scored by using an inflammation scale from - to ++, with - indicating absent inflammation, + showing mild

Table 1. *In vitro* growth-inhibitory activity of SN-38, NK012, CPT-11, and CDDP in human SCLC cells

Cell line	IC_{50} (μmol/L)			
	SN-38	NK012	CPT-11	CDDP
SBC-3/VEGF	0.00330 ± 0.00210	0.00365 ± 0.00005	1.11 ± 0.29	2.21 ± 0.36
SBC-3/Neo	0.00872 ± 0.00063	0.0101 ± 0.0006	5.05 ± 0.08	12.8 ± 1.5
H69	0.0205 ± 0.0195	0.0417 ± 0.0052	22.2 ± 5.9	6.23 ± 0.33
H82	0.00716 ± 0.00079	0.00998 ± 0.00328	1.98 ± 0.55	4.08 ± 3.79

inflammation predominantly infiltrated with lymphocytes, and ++ indicating active inflammation infiltrated with lymphocytes and neutrophils.

Distribution of NK012 or CPT-11 in small intestine by fluorescence microscopy. NK012 or CPT-11 was administered to female BALB/c nude mice at 20 or 30 mg/kg on day 0, respectively. Mice were sacrificed 1, 6, 24, and 72 h after drug injection, and the small intestine was excised at the middle portion and embedded in an OCT compound (Sakura Finetechnochemical Co. Ltd.) and frozen at -80°C. Tissue sections (5 μm thick) were prepared using a cryostatic microtome (Tissue-Tek Cryo3, Sakura Finetechnochemical). Frozen sections were examined under a fluorescence microscope (Biorevo, Keyence) at a 358-nm excitation wavelength and a 461-nm emission wavelength to evaluate NK012 or CPT-11 distribution in the small intestine. Because formulations containing SN-38 bound via ester bonds possess a particular fluorescence, both NK012 and CPT-11 were detected under the same fluorescence conditions.

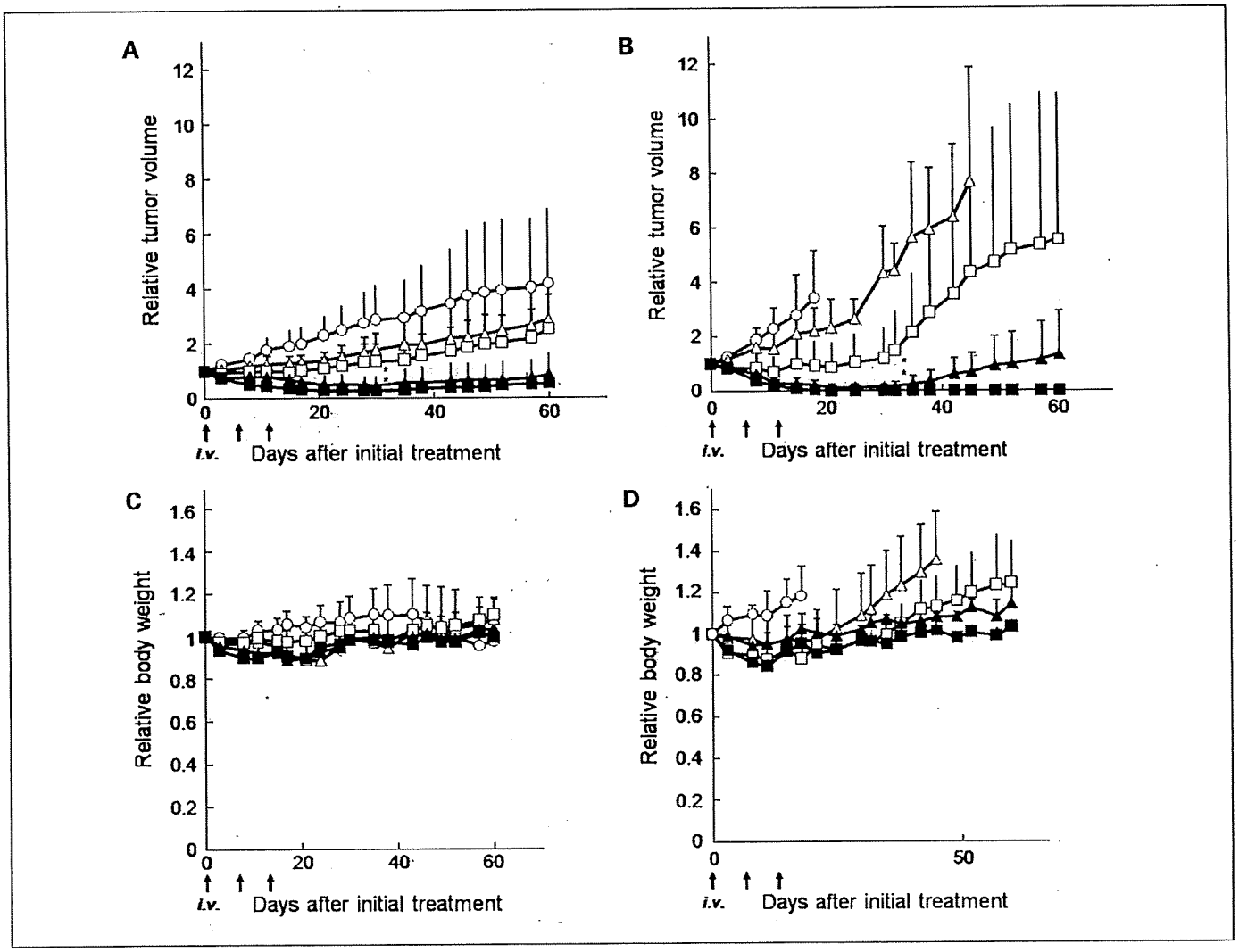

Fig. 1. Growth inhibitory effects of NK012/CDDP and CPT-11/CDDP on SBC-3/Neo and SBC-3/VEGF tumor xenografts. *A* and *B*, RTV in mice treated with NK012/CDDP or CPT-11/CDDP. SBC-3/Neo (*A* and *C*) and SBC-3/VEGF (*B* and *D*) tumors were inoculated s.c. into the flank of mice, as described in Materials and Methods. CPT-11 (10 mg/kg/d; Δ), CPT-11 (22 mg/kg/d; □), NK012 (5 mg/kg/d; ▲), or NK012 (10 mg/kg/d; ■) combined with CDDP (2.5 mg/kg/d) were i.v. administered on days 0, 7, and 14. ○, NaCl solution (0.9%) was i.v. administered as normal control. *Points,* mean; *bars,* SD. *, $P < 0.05$. *C* and *D*, treatment-related BW loss occurred in mice treated with NK012/CDDP and CPT-11/CDDP. *Points,* mean; *bars,* SD.

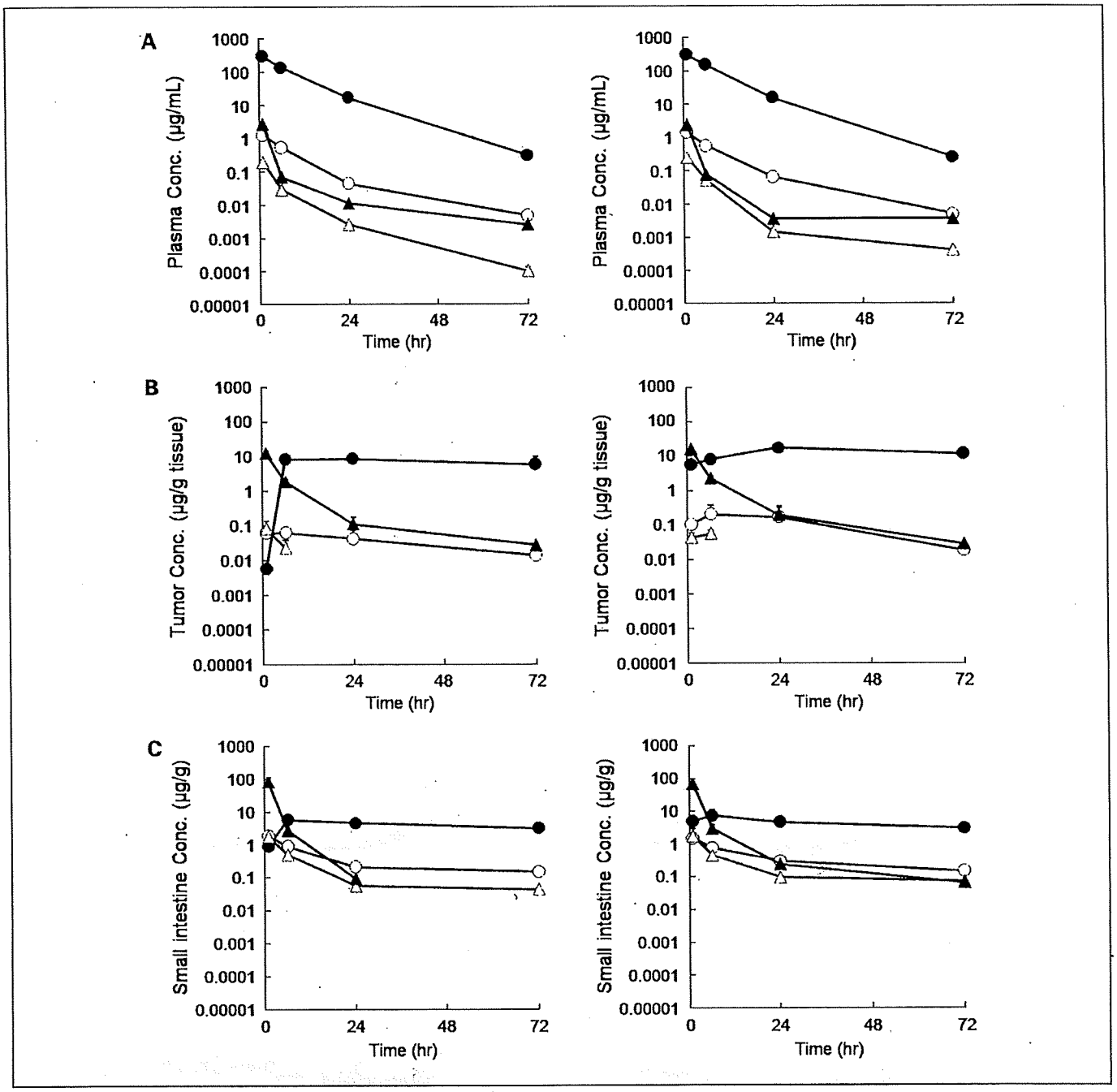

Fig. 2. Plasma, tumor, and small intestine concentrations of NK012, CPT-11, and free SN-38. Plasma (*A*), tumor (*B*), and small intestine (*C*) distribution of NK012, CPT-11, and free SN-38 after i.v. administration of CPT-11 (30 mg/kg) combined with CDDP (2.5 mg/kg) or NK012 (20 mg/kg) combined with CDDP (2.5 mg/kg). Left, SBC-3/Neo; right, SBC-3/VEGF. ●, polymer-bound SN-38; ○, free SN-38 (polymer-unbound SN-38); Δ, SN-38 converted from CPT-11; ▲, CPT-11.

Statistical analysis. Data were analyzed with Student's *t* test when groups showed equal variances (*F* test) or with Welch's test when they showed unequal variances (*F* test). $P < 0.05$ was considered significant. All statistical tests were two sided, and data were expressed as mean ± SD.

Results

Cellular sensitivity of SCLC cells to NK012, CPT-11, SN-38, and CDDP. The IC_{50} values of NK012 for the SCLC cell lines ranged from 0.004 μmol/L (SBC-3/VEGF) to 0.041 μmol/L (H69; Table 1). The cytotoxic effects of NK012 were 198- to 532-fold higher than those of CPT-11, whereas those of NK012 were 1.10- to 2.00-fold lower than those of SN-38. These features were comparable with those reported previously (12, 13).

The molar ratios of NK012 to CDDP of 1:600 in SBC-3/VEGF, 1:120 in SBC-3/Neo, 1:150 in H69, and 1:400 in H82 were used for the drug combination studies based on the IC_{50} values of NK012 and CDDP (Table 1). The synergic to additive

effect between NK012 and CDDP was observed in these SCLC cell lines (data not shown).

Antitumor activity of NK012/CDDP and CPT-11/CDDP against SBC-3/Neo and SBC-3/VEGF tumors. SBC-3/Neo and SBC-3/VEGF tumors treated with 5 mg/kg/d NK012 plus 2.5 mg/kg/d CDDP were significantly smaller than those treated with 10 mg/kg/d CPT-11 plus 2.5 mg/kg/d CDDP on day 30 (P = 0.0024, SBC-3/Neo; P = 0.0437, SBC-3/VEGF). Moreover, both tumors treated with 10 mg/kg/d NK012 plus 2.5 mg/kg/d CDDP were significantly smaller than those treated with 22 mg/kg/d CPT-11 plus 2.5 mg/kg/d CDDP on day 30 (P = 0.0058, SBC-3/Neo; P = 0.0478, SBC-3/VEGF; Fig. 1A and B). Although treatment-related BW loss was observed in mice treated with each drug combination, BW recovered to the normal level in each group by day 30 (Fig. 1C and D). A stronger antitumor activity against SBC-3/VEGF tumors was observed than against SBC-3/Neo tumors. The complete response rates achieved with 10 mg/kg/d NK012 plus 2.5 mg/kg/d CDDP were 100% and 0% for SBC-3/VEGF and SBC-3/Neo, respectively. These results further confirm our previous findings that a more potent antitumor effect of NK012 is observed in highly vascularized tumors (12).

Pharmacokinetics of NK012 and CPT-11 after NK012/CDDP and CPT-11/CDDP administration in mice bearing SBC-3/Neo or SBC-3/VEGF tumors. After CPT-11/CDDP injection, the plasma concentrations of CPT-11 and SN-38 converted from CPT-11 decreased rapidly within 6 hours in a log-linear fashion (Fig. 2A). Those of NK012 (polymer-bound SN-38) and SN-38 released from NK012 decreased more gradually (Fig. 2A). As for the CPT-11 and free SN-38 concentrations in the SBC-3/Neo and SBC-3/VEGF tumors, they decreased rapidly within 6 hours, and almost no SN-38 converted from CPT-11 was detected at 24 hours in both tumors (Fig. 2B). In the case of NK012/CDDP administration, free SN-38 released from NK012 could be detected in the tumors even at 72 hours after administration (Fig. 2B). In contrast to the case of CPT-11/CDDP administration, the concentrations of free SN-38 released from NK012 were higher in the SBC-3/VEGF tumors than in the SBC-3/Neo tumors at any time point during the observation period (significant at 1 hour; P = 0.013).

Free SN-38 concentrations in the small intestine after NK012/CDDP or CPT-11/CDDP administration were still detectable up to 72 hours in a similar fashion. CPT-11 concentrations 1 hour after CPT-11/CDDP administration were significantly higher than NK012 concentrations after NK012/CDDP administration (P = 0.0056, SBC-3/Neo; P = 0.017, SBC-3/VEGF; Fig. 2C).

These kinetic profiles in liver, spleen, lung, and kidney of free SN-38 after NK012/CDDP or CPT-11/CDDP administration were almost similar to those of NK012 or CPT-11 when administered as a single agent, as described (data not shown; ref. 12).

Intestinal toxicity of NK012, NK012/CDDP, CPT-11, and CPT-11/CDDP. Pathologic findings and characteristic mucosal changes are shown in Table 2 and Fig. 3. The small intestinal mucosa of mice in the CPT-11 or CPT-11/CDDP treatment group showed fibrotic changes, and active inflammation with cellular invasion, healed erosion, deformed glandular alignment, and glandular duct disappearance were also found. On the other hand, the small intestinal mucosa of mice in the NK012/CDDP treatment group showed only mild shortening and decreased number of villi or mild inflammatory cell invasion.

We next analyzed the concentrations of NK012, CPT-11, and free SN-38 in the feces. CPT-11 concentrations at 1 hour were significantly higher than NK012 concentrations (P = 0.0021) and decreased rapidly within 24 hours but remained detectable up to 72 hours. On the other hand, NK012 (polymer-bound SN-38) could be detected at a low concentration from 72 hours (Fig. 4A). To evaluate drug distribution over time, sections of the small intestine treated with NK012 or CPT-11 were examined by fluorescence microscopy. In the sections of CPT-11–treated small intestine, strong fluorescence originating from CPT-11 was detected in the epithelium of the small intestine, whereas weaker fluorescence originating from NK012 was distributed uniformly in the mucosal interstitium (Fig. 4B).

Discussion

Here, we compared the antitumor activity of NK012/CDDP with CPT-11/CDDP, the latter being one of the most active regimens against SCLC and NSCLC. The present data showed that when NK012/CDDP was administered, NK012 effectively accumulated in SBC-3/VEGF tumors and sufficiently exerted antitumor effects. This suggests that CDDP did not affect the permeability of tumor vessels and NK012 retention in the tumors. Hasegawa et al. (29) reported that 17 of 24 patients showed positive immunoreactivity for the VEGF protein in tumor specimens and that elevated serum VEGF levels were

Table 2. Pathologic analysis of small intestine after i.v. administration of drugs

Case no.	Treatment group	Site	Fibrosis	Inflammation	
1	Control	Jejunum	-	-	
	Control	Ileum	-	-	
2	Control	Jejunum	-	-	
	Control	Ileum	-	-	
3	Control	Jejunum	-	-	
	Control	Ileum	-	-	
4	CPT-11	Jejunum	+	+	
	CPT-11	Ileum	+	++	Erosion
5	CPT-11	Jejunum	+	+	Edema
	CPT-11	Ileum	-	-	
6	CPT-11	Jejunum	-	-	
	CPT-11	Ileum	+	+	Erosion
7	CDDP + CPT	Jejunum	+	+	
	CDDP + CPT	Ileum	-	-	
8	CDDP + CPT	Jejunum	+	+	
	CDDP + CPT	Ileum	-	+	
9	CDDP + CPT	Jejunum	+	+	
	CDDP + CPT	Ileum	-	-	
10	NK012	Jejunum	-	-	
	NK012	Ileum	-	-	
11	NK012	Jejunum	-	-	
	NK012	Ileum	-	-	
12	NK012	Jejunum	-	-	
	NK012	Ileum	-	+	
13	CDDP + NK012	Jejunum	-	+	
	CDDP + NK012	Ileum	-	+	
14	CDDP + NK012	Jejunum	-	+	
	CDDP + NK012	Ileum	-	-	
15	CDDP + NK012	Jejunum	-	+	
	CDDP + NK012	Ileum	-	-	

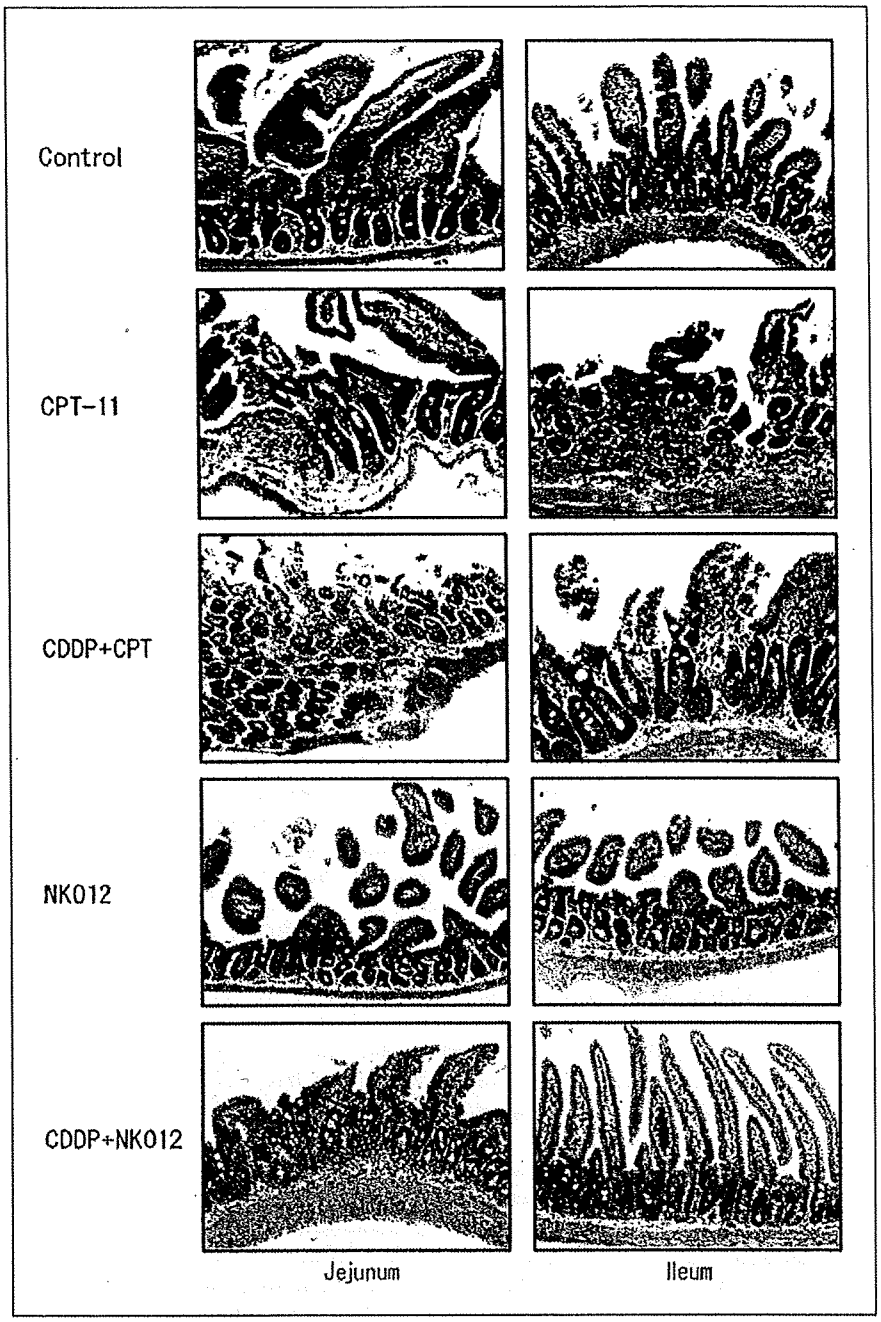

Fig. 3. Pathologic findings and characteristic mucosal changes in mouse. Jejunal and ileal mucosae from mice treated with NaCl solution (0.9%) as control, CPT-11 (22 mg/kg), CPT-11 (22 mg/kg) combined with CDDP (2.5 mg/kg), NK012 (10 mg/kg), or NK012 (10 mg/kg) combined with CDDP (2.5 mg/kg) on days 0, 7, and 14 were examined on day 28 after drug injections. The jejunal mucosa of mice in the CPT-11 treatment group showed healed erosion with fibrotic changes and lymphocytic invasion. Glandular arrangement was severely altered. Active inflammation with inflammatory cell invasion and disappearance of gland ducts were observed on the ileal mucosa in the CPT-11 treatment group. In the CPT-11/CDDP treatment group, the jejunal mucosa also showed healed erosion with scar-like fibrotic growth and mild inflammatory cell invasion into the ileal mucosa. The jejunal and ileal mucosae in the NK012 treatment group and the ileal mucosa in the NK012/CDDP treatment group were almost the same as those in the control group, that is, without inflammatory changes. The jejunal mucosa in the NK012/CDDP treatment group showed mild shortening and decreased number of villi or mild inflammatory cell invasion.

associated with poor outcome in SCLC. As for NSCLC, it was reported that the percentage of VEGF-positive cells was 52 ± 33% (95% confidence interval, 41-64%; median, 70%), and this value showed a positive association with high vascular grade ($P = 0.008$) and poor survival ($P = 0.04$; ref. 30). Taking all data together, NK012/CDDP may therefore be clinically effective against lung cancers, particularly those with high VEGF production.

Pathologic examinations were also conducted to evaluate changes in the small intestinal mucosa on day 14 after treatment. This is because diarrhea is one of the clinical dose-limiting toxicities of CPT-11, and epithelial apoptosis was reported as a mucosal change induced by CPT-11 (31). This pathologic change was observed on day 6 after i.p. administration of 100 mg/kg CPT-11 daily for 4 days. We found that the CPT-11–induced mucosal change was mainly fibrosis considered to be a form of recovery change from erosion. On the other hand, the small intestinal mucosa of the mice in the NK012/CDDP treatment group showed only mild shortening and decreased number of villi or mild inflammatory cell invasion. On comparison of these changes with those caused by CDDP (31), it was found that such alterations were mainly induced by CDDP rather than NK012.

A portion of SN-38 converted from CPT-11 undergoes subsequent conjugation as induced by UDP-glucuronyltransferase to form SN-38 β-glucuronide (SN-38-Glu; ref. 32). CPT-11, SN-38, and SN-38-Glu are excreted into the bile and then reach the small intestinal lumen (32, 33). SN-38-Glu is

deconjugated in the cecum and colon to regenerate SN-38 through bacterial β-glucuronidase (34). In this study, CPT-11 was excreted into feces much more than NK012 and a high CPT-11 concentration was detected in the small intestinal epithelium. It is speculated that the highly excreted CPT-11 is reabsorbed in the small intestinal epithelium and converted to SN-38 to cause damage to the intestinal mucosa. On the other hand, NK012 was uniformly distributed in the mucosal interstitium at a lower concentration, which may be related to the less mucosal damage and diarrhea than those induced by CPT-11, although NK012 was observed for longer period than CPT-11. About other toxic effects including bone marrow, liver,

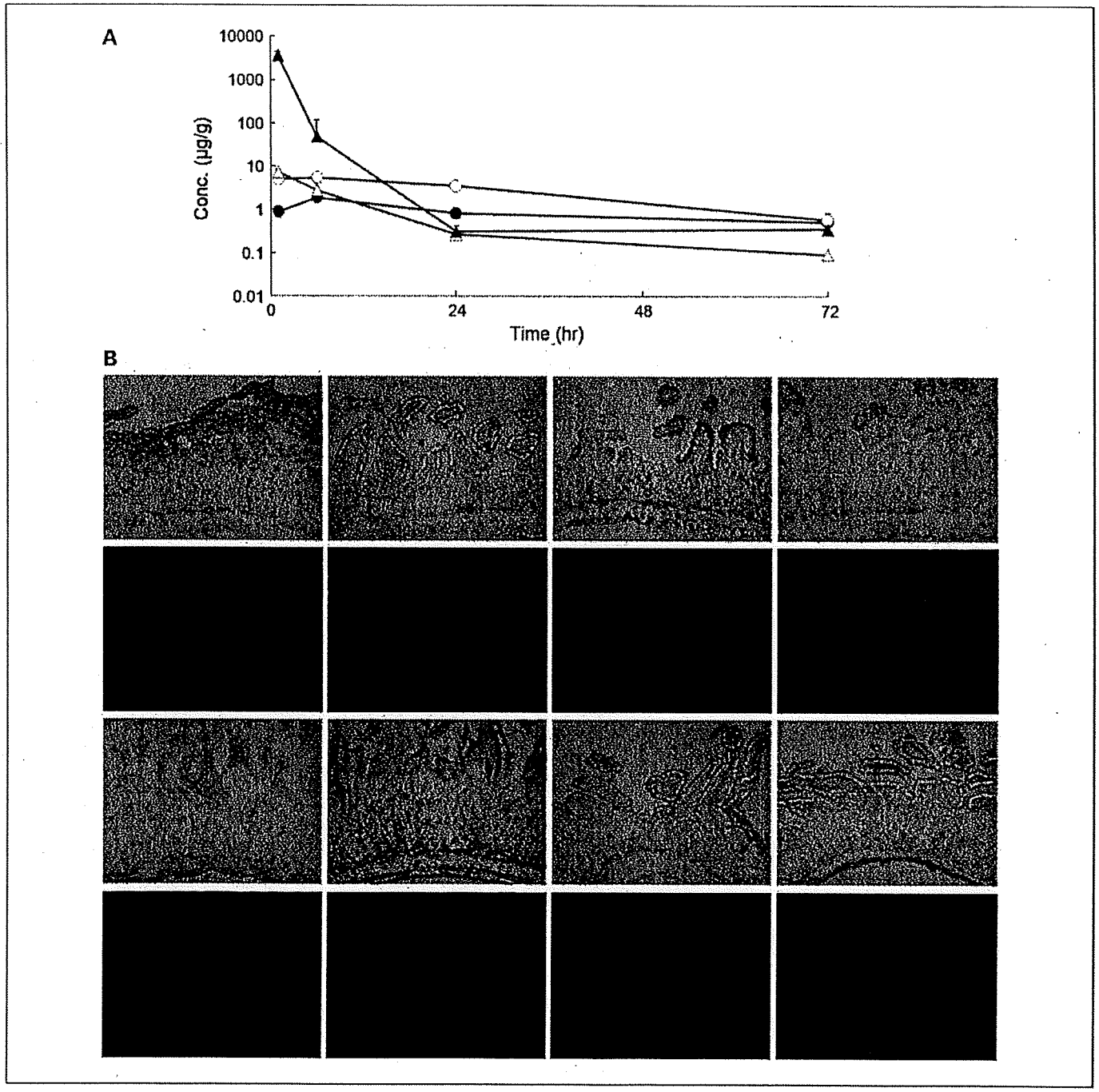

Fig. 4. Fecal concentrations of NK012, CPT-11, and free SN-38, and NK012 or CPT-11 distribution in the small intestine. *A*, distribution of NK012, CPT-11, and free SN-38 after i.v. administration of CPT-11 (30 mg/kg) or NK012 (20 mg/kg). ●, polymer-bound SN-38; ○, free SN-38 (polymer-unbound SN-38); △, SN-38 converted from CPT-11; ▲, CPT-11. *B*, small intestines were excised 1, 6, 24, and 72 h after i.v. administration of CPT-11 (30 mg/kg) or NK012 (20 mg/kg). Frozen sections were examined under a fluorescence microscope at a 358-nm excitation wavelength and a 461-nm emission wavelength. NK012 and CPT-11 were visualized as blue. The first or third columns are a bright-field image and the second or forth columns are a fluorescence image. Sections of small intestines were most well visualized in bright field. First, second, third, and fourth lines from the left side are images obtained 1, 6, 24, and 72 h after drug administration, respectively. CPT-11 was strongly distributed in the epithelium of the small intestine, whereas NK012 tended to be distributed weakly and uniformly in the mucosal interstitium.

and kidney toxicities, there was no significant difference between NK012/CDDP and CPT-11/CDDP in the present treatment schedule (data not shown).

In conclusion, NK012/CDDP showed a significantly higher antitumor activity with no severe diarrhea toxicity than CPT-11/CDDP, one of the most active regimens against SCLC and NSCLC. The present data suggest the clinical evaluation of NK012/CDDP in patients with SCLC and NSCLC.

Disclosure of Potential Conflicts of Interest

No potential conflicts of interest were disclosed.

Acknowledgments

We thank N. Mie and M. Ohtsu for their technical assistance and K. Shiina and K. Abe for their secretarial assistance.

References

1. Argiris A, Murren JR. Advances in chemotherapy for small cell lung cancer: single-agent activity of newer agents. Cancer J 2001;7:228–35.
2. Bodurka DC, Levenback C, Wolf JK, et al. Phase II trial of irinotecan in patients with metastatic epithelial ovarian cancer or peritoneal cancer. J Clin Oncol 2003;21:291–7.
3. Cunningham D, Pyrhonen S, James RD, et al. Randomised trial of irinotecan plus supportive care versus supportive care alone after fluorouracil failure for patients with metastatic colorectal cancer. Lancet 1998;352:1413–8.
4. Negoro S, Masuda N, Takada Y, et al. Randomised phase III trial of irinotecan combined with cisplatin for advanced non-small-cell lung cancer. Br J Cancer 2003;88:335–41.
5. Mathijssen RH, van Alphen RJ, Verweij J, et al. Clinical pharmacokinetics and metabolism of irinotecan (CPT-11). Clin Cancer Res 2001;7:2182–94.
6. Rothenberg ML, Kuhn JG, Burris HA III, et al. Phase I and pharmacokinetic trial of weekly CPT-11. J Clin Oncol 1993;11:2194–204.
7. Slatter JG, Schaaf LJ, Sams JP, et al. Pharmacokinetics, metabolism, and excretion of irinotecan (CPT-11) following i.v. infusion of [(14)C]CPT-11 in cancer patients. Drug Metab Dispos 2000;28:423–33.
8. Dvorak HF, Nagy JA, Dvorak JT, Dvorak AM. Identification and characterization of the blood vessels of solid tumors that are leaky to circulating macromolecules. Am J Pathol 1988;133:95–109.
9. Maeda H, Matsumura Y. Tumoritropic and lymphotropic principles of macromolecular drugs. Crit Rev Ther Drug Carrier Syst 1989;6:193–210.
10. Matsumura Y, Maeda H. A new concept for macromolecular therapeutics in cancer chemotherapy: mechanism of tumoritropic accumulation of proteins and the antitumor agent smancs. Cancer Res 1986; 46:6387–92.
11. Matsumura Y, Maruo K, Kimura M, Yamamoto T, Konno T, Maeda H. Kinin-generating cascade in advanced cancer patients and *in vitro* study. Jpn J Cancer Res 1991;82:732–41.
12. Koizumi F, Kitagawa M, Negishi T, et al. Novel SN-38-incorporating polymeric micelles, NK012, eradicate vascular endothelial growth factor-secreting bulky tumors. Cancer Res 2006;66:10048–56.
13. Nakajima TE, Yasunaga M, Kano Y, et al. Synergistic antitumor activity of the novel SN-38-incorporating polymeric micelles, NK012, combined with 5-fluorouracil in a mouse model of colorectal cancer, as compared with that of irinotecan plus 5-fluorouracil. Int J Cancer 2008;122:2148–53.
14. Sumitomo M, Koizumi F, Asano T, et al. Novel SN-38-incorporated polymeric micelle, NK012, strongly suppresses renal cancer progression. Cancer Res 2008;68:1631–5.
15. Saito Y, Yasunaga M, Kuroda J, Koga Y, Matsumura Y. Enhanced distribution of NK012, a polymeric micelle-encapsulated SN-38, and sustained release of SN-38 within tumors can beat a hypovascular tumor. Cancer Sci 2008;99:1258–64.
16. Eguchi Nakajima T, Yanagihara K, Takigahira M, et al. Antitumor effect of SN-38-releasing polymeric micelles, NK012, on spontaneous peritoneal metastases from orthotopic gastric cancer in mice compared with irinotecan. Cancer Res 2008;68: 9318–22.
17. Kuroda J, Kuratsu J, Yasunaga M, Koga Y, Saito Y, Matsumura Y. Potent antitumor effect of SN-38-incorporating polymeric micelle, NK012, against malignant glioma. Int J Cancer 2009;124:2505–11.
18. Fukuda M, Nishio K, Kanzawa F, et al. Synergism between cisplatin and topoisomerase I inhibitors, NB-506 and SN-38, in human small cell lung cancer cells. Cancer Res 1996;56:789–93.
19. Noda K, Nishiwaki Y, Kawahara M, et al. Irinotecan plus cisplatin compared with etoposide plus cisplatin for extensive small-cell lung cancer. N Engl J Med 2002;346:85–91.
20. Ohe Y, Ohashi Y, Kubota K, et al. Randomized phase III study of cisplatin plus irinotecan versus carboplatin plus paclitaxel, cisplatin plus gemcitabine, and cisplatin plus vinorelbine for advanced non-small-cell lung cancer: Four-Arm Cooperative Study in Japan. Ann Oncol 2007;18:317–23.
21. Ohe Y, Sasaki Y, Shinkai T, et al. Phase I study and pharmacokinetics of CPT-11 with 5-day continuous infusion. J Natl Cancer Inst 1992;84:972–4.
22. Masuda N, Fukuoka M, Kusunoki Y, et al. CPT-11: a new derivative of camptothecin for the treatment of refractory or relapsed small-cell lung cancer. J Clin Oncol 1992;10:1225–9.
23. Ohno R, Okada K, Masaoka T, et al. An early phase II study of CPT-11: a new derivative of camptothecin, for the treatment of leukemia and lymphoma. J Clin Oncol 1990;8:1907–12.
24. Kato K, Hamaguchi T, Shirao K, et al. Interim analysis of phase I study of NK012, polymer micelle SN-38, in patients with advanced cancer [abstract 485]. Proc Am Soc Clin Oncol 2008.
25. Burris III HA, Infante JR, Spigel DR, et al. A phase I dose-escalation study of NK012 [abstract 2538]. Proc Am Soc Clin Oncol 2008.
26. Natsume T, Watanabe J, Koh Y, et al. Antitumor activity of TZT-1027 (Soblidotin) against vascular endothelial growth factor-secreting human lung cancer *in vivo*. Cancer Sci 2003;94:826–33.
27. Chou TC, Talalay P. Quantitative analysis of dose-effect relationships: the combined effects of multiple drugs or enzyme inhibitors. Adv Enzyme Regul 1984; 22:27–55.
28. Kudoh S, Takada M, Masuda N, et al. Enhanced antitumor efficacy of a combination of CPT-11, a new derivative of camptothecin, and cisplatin against human lung tumor xenografts. Jpn J Cancer Res 1993;84: 203–7.
29. Hasegawa Y, Takanashi S, Okudera K, et al. Vascular endothelial growth factor level as a prognostic determinant of small cell lung cancer in Japanese patients. Intern Med 2005;44:26–34.
30. Giatromanolaki A, Koukourakis MI, Kakolyris S, et al. Vascular endothelial growth factor, wild-type p53, and angiogenesis in early operable non-small cell lung cancer. Clin Cancer Res 1998; 4:3017–24.
31. Ikuno N, Soda H, Watanabe M, Oka M. Irinotecan (CPT-11) and characteristic mucosal changes in the mouse ileum and cecum. J Natl Cancer Inst 1995;87: 1876–83.
32. Atsumi R, Suzuki W, Hakusui H. Identification of the metabolites of irinotecan, a new derivative of camptothecin, in rat bile and its biliary excretion. Xenobiotica 1991;21:1159–69.
33. Chu XY, Kato Y, Sugiyama Y. Multiplicity of biliary excretion mechanisms for irinotecan, CPT-11, and its metabolites in rats. Cancer Res 1997;57:1934–8.
34. Takasuna K, Hagiwara T, Hirohashi M, et al. Involvement of β-glucuronidase in intestinal microflora in the intestinal toxicity of the antitumor camptothecin derivative irinotecan hydrochloride (CPT-11) in rats. Cancer Res 1996;56:3752–7.

Cancer Therapy: Preclinical

Clinical Cancer Research

Antitumor Effect of NK012, a 7-Ethyl-10-Hydroxycamptothecin–Incorporating Polymeric Micelle, on U87MG Orthotopic Glioblastoma in Mice Compared with Irinotecan Hydrochloride in Combination with Bevacizumab

Jun-ichiro Kuroda[1,2], Jun-ichi Kuratsu[2], Masahiro Yasunaga[1], Yoshikatsu Koga[1], Hirotsugu Kenmotsu[1], Takashi Sugino[3], and Yasuhiro Matsumura[1]

Abstract

Purpose: To clarify the effect of bevacizumab on NK012 therapy in mice bearing U87MG glioblastoma orthotopic xenografts in comparison with the combination therapy of irinotecan hydrochloride (CPT-11) with bevacizumab.

Experimental Design: NK012 at 7-ethyl-10-hydroxycamptothecin (SN-38) equivalent dose of 30 mg/kg was administered intravenously three times every 4 days with or without bevacizumab. CPT-11 at 66.7 mg/kg was administered intravenously three times every 4 days or CPT-11 at 40 mg/kg/d over 5 consecutive days with or without bevacizumab. Bevacizumab was administered intraperitoneally six times every 4 days in each experiment. *In vivo* antitumor effects were evaluated by bioluminescence imaging, histopathologic evaluation, and immunohistochemistry. To evaluate interaction with bevacizumab, free SN-38 concentration in tumor tissues was examined by high-performance liquid chromatography.

Results: CPT-11 in combination with bevacizumab showed significantly more potent antitumor activity and longer survival than CPT-11 monotherapy ($P < 0.05$). However, there was no difference between NK012 monotherapy and NK012 in combination with bevacizumab. Concentration of free SN-38 released from NK012 in tumor tissue decreased in combination with bevacizumab ($P = 0.027$). NK012 monotherapy or NK012 with bevacizumab showed potent antitumor activity and longer survival than any dosing method of CPT-11 in combination with bevacizumab ($P < 0.05$). Orthotopic tumors treated with NK012 showed decreased tumor cellularity and lower Ki-67 index ($P < 0.001$) relative to those treated with CPT-11/bevacizumab.

Conclusions: The present study using orthotopic glioblastoma model in mice may warrant further preclinical evaluation of NK012 before conducting the clinical trial of the drug, because the antitumor activity of NK012 monotherapy was superior to the combination therapy of CPT-11 with bevacizumab.

Clin Cancer Res; 16(2); 521–9. ©2010 AACR.

Malignant glioma, such as glioblastoma multiforme and anaplastic astrocytoma, are the most commonly occurring primary malignant brain tumors, and glioblastoma multiforme is well known as a typical hypervascular tumor with a high expression level of vascular endothelial growth factor (VEGF; ref. 1). Currently, glioblastoma multiforme patients have a mean survival time of only 50 weeks following the standard treatment consisting of surgical and adjuvant therapies (2). However, a recent phase III randomized trial for newly diagnosed glioblastoma multiforme showed that radiation therapy with concurrent temozolomide treatment followed by 6 months of temozolomide treatment was superior to radiation therapy alone in terms of overall survival (3). Furthermore, several clinical trials have shown that the median survival time of patients with recurrence was only 30 weeks (4). Therefore, a novel antitumor agent based on a new approach for the recurrent malignant glioma is eagerly awaited.

7-Ethyl-10-hydroxycamptothecin (SN-38) is a broad-spectrum anticancer agent targeting DNA topoisomerase I. Irinotecan hydrochloride (CPT-11), a prodrug of SN-38, shows some antitumor activity in patients with recurrent glioblastoma multiforme, with response rates of 0 to 17% in several trials (5–8). CPT-11 single-agent chemotherapy activity is thus similar to that of other agents used for

Authors' Affiliations: [1]Investigative Treatment Division, Research Center for Innovative Oncology, National Cancer Center Hospital East, Kashiwa, Japan; [2]Department of Neurosurgery, Faculty of Medical and Pharmaceutical Sciences, Kumamoto University, Kumamoto, Japan; and [3]Department of Pathology, Fukushima Medical University School of Medicine, Fukushima, Japan

Corresponding Author: Yasuhiro Matsumura, Investigative Treatment Division, Research Center for Innovative Oncology, National Cancer Center Hospital East, 6-5-1 Kashiwanoha, Kashiwa 277-8577, Japan. Phone: 81-4-7134-6857; Fax: 81-4-7134-6857; E-mail: yhmatsum@east.ncc.go.jp.

doi: 10.1158/1078-0432.CCR-09-2393

Translational Relevance

A recent phase II trial for recurrent glioblastoma multiforme showed that irinotecan hydrochloride (CPT-11) combined with bevacizumab is a promising and unprecedentedly effective treatment against the recurrent glioblastoma multiforme. However, there may be an increasing risk of developing venous thrombotic disease and intracranial hemorrhage with this combination therapy. The 7-ethyl-10-hydroxycamptothecin–incorporating polymeric micelle NK012 has been shown to have significant antitumor activity against several cancer mouse models compared with CPT-11. Two phase I trials in Japan and the United States showed that patients treated with NK012 did not develop grade 3/4 diarrhea, one of the major adverse effects of CPT-11. Here, NK012 showed potent antitumor activity and longer survival than CPT-11 in combination with bevacizumab in glioblastoma multiforme orthotopic tumor in mice. These results warrant clinical evaluation in patients with malignant glioma.

recurrent glioblastoma multiforme (7). Meanwhile, glioblastoma cells express high levels of VEGF *in situ*. Accordingly, antiangiogenic strategies may be a promising approach for malignant gliomas hypervascular in nature. A recent phase II trial for recurrent glioblastoma multiforme showed that CPT-11 combined with bevacizumab, an anti-VEGF monoclonal IgG1 antibody, is a promising and unprecedentedly effective treatment against the recurrent malignant glioma with a 6-month progression-free survival rate of 46% and a 6-month overall survival rate of 77% (9, 10). On the other hand, there may be an increased risk of developing venous thromboembolic disease and intracranial hemorrhage with this combination therapy. Therefore, it is reasonable to develop other available treatment modalities by which cytotoxic drugs can exert more potent antitumor activity to their full potential with modest adverse effects and thereby reasonably prolong the overall survival of recurrent glioblastoma multiforme patients.

NK012, a SN-38–incorporating polymeric micelle, is a prodrug of SN-38 similar to CPT-11. Polymer-conjugated drugs categorized under drug delivery system agents are favorably extravasated from tumor vessels into the interstitium of tumors due to the enhanced permeability and retention effect (11, 12). The enhanced permeability and retention effect is based on the following pathophysiologic characteristics of solid tumor tissues: hypervascularity; incomplete vascular architecture; secretion of vascular permeability factors stimulating extravasation within cancer tissue; and absence of effective lymphatic drainage from the tumors, which impedes the efficient clearance of macromolecules accumulated in solid tumor tissues. Moreover, macromolecules cannot freely leak out from normal vessels; thus, the adverse effect of an anticancer agent can be reduced. Very recently, we showed that NK012 exerted significantly more potent antitumor activity against several kinds of tumors including human glioma in xenograft models (13). In the present study, we report the antitumor activity of NK012 compared with CPT-11 combined with bevacizumab against orthotopic U87MG glioblastoma in nude mice.

Materials and Methods

Drugs. NK012 was supplied by Nippon Kayaku. Lyophilized NK012 was dissolved in sterile distilled water at a concentration of 5 mg/mL (SN-38 equivalent dose) just before administration to mice. The size of NK012 was ~20 nm in diameter with a narrow size distribution (12). CPT-11 was purchased from Yakult Honsha. Bevacizumab was purchased from Chugai Pharmaceutical.

Cell cultures. The human glioblastoma cell line U87MG was obtained directly from the American Type Culture Collection. A U87MG cell line clone stably expressing firefly luciferase named U87MG/Luc was established from polyclonal U87MG/Luc reported previously (13). The sensitivity of U87MG/Luc cells to NK012 and CPT-11 was almost similar to that of parental U87MG cells (data not shown). U87MG/Luc cells were maintained in DMEM supplemented with 10% fetal bovine serum (Cell Culture Technologies), penicillin, streptomycin, and amphotericin B (100 units/mL, 100 μg/mL, and 25 μg/mL, respectively; Sigma) in a humidified atmosphere containing 5% CO_2 at 37°C.

In vivo *orthotopic model and imaging.* Six- to 8-week-old female athymic BALB/c *nu/nu* mice (Charles River Japan) were used for this study. U87MG/Luc cells (5×10^5) suspended in 5 μL PBS were injected into the right frontal lobe of each mouse as described previously (13). *In vivo* bioluminescence imaging studies were done using the Photon Imager animal imaging system (BioSpace). For imaging, mice with intracranial U87MG/Luc tumor were simultaneously anesthetized with isoflurane, and D-luciferin potassium salt (Synchem) was intraperitoneally administered at a dose of 2.5 mg/mouse. For bioluminescence image analysis, regions of interest encompassing the intracranial area of a signal were defined using Photo Vision software (BioSpace), and the total number of photons per minute [counts/min (cpm)] was recorded. The pseudo-color luminescent image represented the spatial distribution of detected photon counts emerging from active luciferase within the animal. All animal procedures were done in compliance with the Guidelines for the Care and Use of Experimental Animals established by the Committee for Animal Experimentation of the National Cancer Center, Japan; these guidelines meet the ethical standards required by law and also comply with the guidelines for the use of experimental animals in Japan.

In vivo *tumor growth inhibition assay.* Eight days after inoculation of U87MG/Luc cells into the right hemisphere of the brain, mice with cpm >2,000 were randomly assigned into eight test groups of five mice

(2,296-15,624 cpm). After the randomization of mice based on cpm, we confirmed that the mean value of cpm was statistically identical between groups.

Treatment was started (day 0; Table 1). *In vivo* bioluminescence imaging was done by Photon Imager and luciferase activity was measured once a week (days 0, 7, 14, 21, 28, and 35). Body weight of each mouse of the treatment experiment was also measured once a week (days 0, 7, 14, 21, 28, and 35), and mortality and morbidity were checked daily from the day of treatment initiation. Simultaneously, to assess the survival of mice with intracranial U87MG/Luc tumor, mice were maintained until each animal showed signs of morbidity (20% weight loss and neurologic deficit), at which point they were sacrificed.

In all groups, the total dose of NK012 and CPT-11 was 90 mg/kg (SN-38 equivalent dose) and 200 mg/kg, respectively. A total dose of 200 mg/kg was shown previously to be the maximum tolerated dose (MTD) of CPT-11 in nude mice (14, 15). As CPT-11 is a schedule-dependent anticancer agent, it was administered under two different treatment regimens (16). Each drug was administered according to the mouse body weight: (*a*) normal 0.9% NaCl solution (q4d × 4, intravenously), (*b*) NK012 (30 mg/kg, q4d × 3, intravenously), (*c*) CPT-11 (66.7 mg/kg, q4d × 3, intravenously), (*d*) CPT-11 (40 mg/kg, qd × 5, intravenously), (*e*) bevacizumab (5 mg/kg, q4d × 6, intraperitoneally), (*f*) NK012 (30 mg/kg, q4d × 3, intravenously) with bevacizumab (5 mg/kg, q4d × 6, intraperitoneally), (*g*) CPT-11 (66.7 mg/kg, q4d × 3, intravenously) with bevacizumab (5 mg/kg, q4d × 6, intraperitoneally), or (*h*) CPT-11 (40 mg/kg, qd × 5, intravenously) with bevacizumab (5 mg/kg, q4d × 6, intraperitoneally) was administered to the mice (Table 1). In the case of combination therapy, drugs were administered concomitantly.

Evaluation of antitumor activity. The antitumor activity of each treatment was evaluated according to three criteria: (*a*) number of tumor regressions, (*b*) tumor growth delay, and (*c*) Kaplan-Meier analysis to determine the effect on the time to morbidity. Decrease >50% of the initial photon count (cpm) was defined as a tumor regression. It had to be observed for at least two consecutive photon-counting events to be retained. Tumor growth delay was defined as the difference in the median time to reach a photon count of 5-fold compared with that of day 0 between the treated group and the control group (14). To evaluate the change in photon count of each treatment group, repeated-measures ANOVA was carried out using the StatView 5.0 software package. $P < 0.05$ was regarded as significant. Statistical differences in the Kaplan-Meier curve of each group were ranked according to the Breslow-Gehan-Wilcoxon test using StatView 5.0.

Immunohistochemistry. Histologic sections were taken from U87MG/Luc orthotopic tumor tissues at day 15 from the initiation of each therapy. The time points for analysis were chosen according to when the best antitumor activity was obtained. The brain was removed from the skull, fixed in buffered 4% paraformaldehyde, embedded in paraffin, and then cut into 3-μm-thick sections. Conventional H&E-stained sections were prepared for general histopathologic evaluation. Immunohistochemistry was done using antibodies to human Ki-67 (BD Pharmingen), human VEGF (Santa Cruz Biotechnology), and mouse CD34 (MEC 14.7; Abcam). For antigen retrieval, sections were autoclaved in Dako REAL Target Retrieval Solution (Dako Denmark). Detection was done by Vectastain Elite avidin-biotin complex kit (Vector Laboratories) for CD34 and EnVision$^+$ system labeled polymer-horseradish peroxidase anti-mouse (DakoCytomation) for Ki-67 and anti-rabbit for VEGF. The proliferation index was evaluated by counting Ki-67$^+$ cells per 1,000 tumor cells using ImagePro Plus analysis software. VEGF immunoreactivity area was quantified using the analysis software BZ Analyzer (Keyence) with a constant color threshold in 10 high-power fields per slide (×400) and is given in percent of positive area in field of view. Tumor vascularity was assessed by counting CD34$^+$ microvessels in 10 high-power fields per slide (×400). The small intestine was sampled at 5 cm from the pylolic part for the jejunum and 5 cm

Table 1. Activity of three anticancer drugs against orthotopic U87MG xenografts

Treatment course	Dose (mg/kg/d)	Schedule	Total dose (mg/kg)	No. animals/ group	Maximum body weight loss (%)	Toxic death	Tumor regression	Tumor growth delay (d)	Median overall survival (d)
Control	—	—	—	5	—	—	—	—	29
NK012	30	q4d × 3	90	5	3.8	0	3	>18	48
CPT-11	66.7	q4d × 3	200	5	6.6	0	0	8	36
CPT-11	40	qd × 5	200	5	2	0	1	8	34
Bevacizumab	5	q4d × 6	30	5	1.9	0	0	4	40
NK012/bevacizumab	30/5	q4d × 3/q4d × 6	90/30	5	0.9	0	1	12	46
CPT-11/bevacizumab	66.7/5	q4d × 3/q4d × 6	200/30	5	0	0	2	7	40
CPT-11/bevacizumab	40/5	qd × 5/q4d × 6	200/30	5	0.7	0	2	8	41

NOTE: Maximum body weight loss (days 0-28).

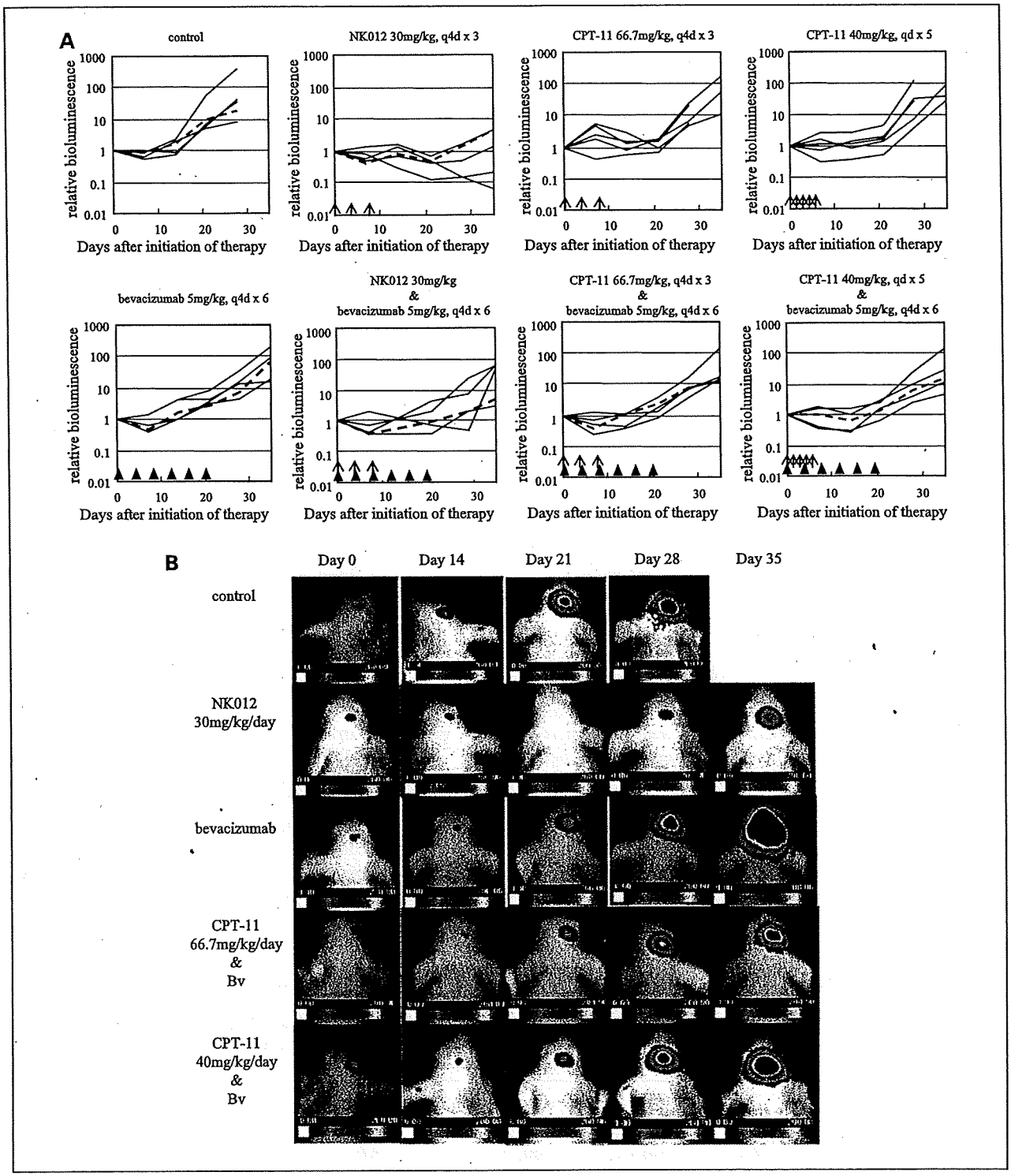

Fig. 1. Effects of NK012 and CPT-11 in U87MG/Luc mouse models. Cells were injected intracranially in athymic mice. Treatments were initiated 8 d after tumor inoculation with NK012, 30 mg/kg intravenously, thrice every 4 d; CPT-11, 67 mg/kg intravenously, thrice every 4 d; CPT-11, 40 mg/kg intravenously, daily over 5 consecutive d; bevacizumab, 5 mg/kg intraperitoneally, six times every 4 d; or both modalities and 0.9% NaCl solution control. †, NK012 or CPT-11 intravenous administration; ▲, bevacizumab intraperitoneal administration. *A*, antitumor activity of NK012 or CPT-11 was evaluated by counting the number of photons using the Photon Imager system. The discontinued lines in some of the graphs represent individuals that died during the experimental course and the subsequent assay was not conducted. The dashed lines correspond to the mice of each therapy expressed in *B*. *B*, images of U87MG/Luc mouse model treated with each regimen taken using the Photon Imager system on days 0, 14, 21, 28, and 35 after the initiation of therapy. Data derived from the same mice are expressed as dashed lines in *A*.

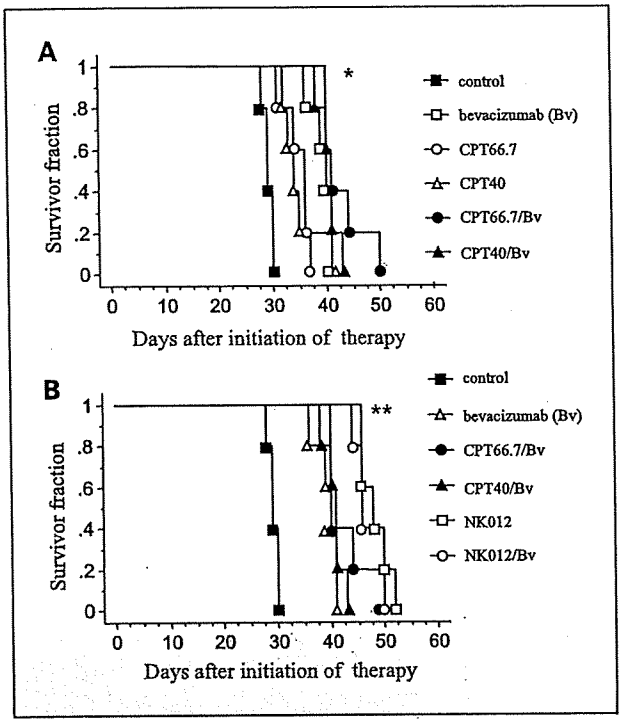

Fig. 2. Survival curves of U87MG/Luc mouse models in each regimen. *A*, ■, 0.9% NaCl solution; □, bevacizumab, 5 mg/kg, q4d × 6; ●, CPT-11, 66.7 mg/kg, q4d × 3 with bevacizumab, 5 mg/kg, q4d × 6; ▲, CPT-11, 40 mg/kg, qd × 5 with bevacizumab, 5 mg/kg, q4d × 6; ○, CPT-11, 66.7 mg/kg, q4d × 3; △, CPT-11, 40 mg/kg, qd × 5. CPT-11/bevacizumab is significantly superior to CPT-11 monotherapy [CPT66.7 versus CPT66.7/bevacizumab ($P < 0.01$) and CPT40 versus CPT40/bevacizumab ($P < 0.05$)]. *B*, □, NK012, 30 mg/kg/d, q4d × 3; ○, NK012, 30 mg/kg/d with bevacizumab, 5 mg/kg, q4d × 6; △, bevacizumab, 5 mg/kg, q4d × 6; ■, 0.9% NaCl solution; ●, CPT-11, 66.7 mg/kg, q4d × 3 with bevacizumab, 5 mg/kg, q4d × 6; ▲, CPT-11, 40 mg/kg, qd × 5 with bevacizumab, 5 mg/kg, q4d × 6. NK012 monotherapy is significantly superior to CPT66.7/bevacizumab ($P < 0.01$) and CPT40/bevacizumab ($P < 0.05$).

from the ileocecal junction for the ileum. Samples were fixed in 10 formalin, embedded in paraffin, sectioned, and stained with H&E. Inflammation was scored by using an inflammation scale from - to ++, with - indicating absent inflammation, + indicating mild inflammation predominantly infiltrated with lymphocytes, and ++ indicating active inflammation infiltrated with lymphocytes and neutrophils. All histopathologic and immunohistologic analysis and interpretation were done directly by an experienced pathologist.

Pharmacokinetics study of NK012 and CPT-11 combined with bevacizumab. Four mice bearing U87MG/Luc tumor per group were used for the biodistribution analysis of NK012 and CPT-11. Twenty-eight days after the intracranial injection of U87MG/Luc cells, NK012 (30 mg/kg) or CPT-11 (66.7 mg/kg) was intravenously administered with or without simultaneous intraperitoneal administration of bevacizumab (5 mg/kg) to the mice. After euthanasia, tumor tissues were obtained at T_{max} of each drug, 12 h after NK012 and 3 h after CPT-11 administration, respectively (12, 13). Each tumor was excised without the adjacent normal brain tissue. The size of tumor was ~5 mm in diameter. The tumor samples were rinsed with 0.9% NaCl solution, mixed with 0.1 mol/L glycine-HCl buffer (pH 3.0)/methanol at 5% (w/w), and then homogenized using Precellys 24 (Bertin Technologies). The samples were vortexed vigorously for 10 s and then filtered through an Ultrafree-MC centrifugal filter device with a cutoff molecular diameter of 0.45 μm (Millipore). We had confirmed that the filtered solution contained only free SN-38. Reverse-phase high-performance liquid chromatography was done at 35°C on a Mightysil RP-18 GP column 150 × 4.6 mm (Kanto Chemical). Fifty microliters of a sample were injected into an Alliance 2795 high-performance liquid chromatography system (Waters Associates) equipped with a Waters 2475 multi λ fluorescence detector. The mobile phase was a mixture of 100 nmol/L ammonium acetate (pH 4.2) and methanol (11:9, v/v). The flow rate was 1.0 mL/min. The content of SN-38 was calculated by measuring the relevant peak area for calibration against the corresponding peak area derived from the CPT internal standard. Peak data were recorded using a chromatography management system (MassLynx version 4.0; Waters Associates).

Statistical analysis. Data were expressed as mean ± SD. Significance of differences was calculated using the unpaired two-tailed *t* test with StatView 5.0. $P < 0.05$ was regarded as statistically significant. Kaplan-Meier analysis was done to determine the antitumor activity of each treatment on the time to morbidity, and statistical differences were ranked accordingto the Breslow-Gehan-Wilcoxon test using StatView 5.0. To evaluate the change in photon count of each treatment group, repeated-measures ANOVA was done.

Results

Antitumor response of U87MG xenograft. NK012 at the MTD (30 mg/kg/d) administered thrice every 4 days proved to be the most active against xenografts, with three tumor regressions and tumor growth delay of >18 days (Table 1). In combination with bevacizumab, CPT-11 at the MTD (66.7 mg/kg/d) administered thrice every 4 days and at the MTD (40 mg/kg/d) administered daily over 5 consecutive days induced two tumor regressions and tumor growth delay of 7 and 8 days, respectively. Without bevacizumab, CPT-11 at the MTD (40 mg/kg) administered daily over 5 consecutive days induced one tumor regression (Table 1). Comparison of the relative photon counts on repeated-measures ANOVA (days 0-28) revealed significant differences in photon counts between mice treated with NK012 and those treated with CPT-11 (66.7 mg/kg/d, q4d × 3) in combination with bevacizumab ($P = 0.02$; Fig. 1A and B). Tendency of differences between mice treated with NK012 and those treated with CPT-11 (40 mg/kg/d, qd × 5) in combination with bevacizumab ($P = 0.14$) was observed (Fig. 1A and B).

The median overall survival time was most prolonged in the NK012 (30 mg/kg/d, q4d × 3) group for 1 week

compared with the CPT-11/bevacizumab group (Table 1). The CPT-11 group with bevacizumab showed longer median overall survival time compared with the CPT-11 monotherapy group with two schedules: 66.7 mg/kg/d, q4d × 3, and 40 mg/kg/d, qd × 5, respectively (Table 1). Kaplan-Meier analysis showed a significant survival benefit of the CPT-11/bevacizumab group compared with the CPT-11 monotherapy (66.7 mg/kg/d, q4d × 3; P = 0.004) and CPT-11 (40 mg/kg/d, qd × 5; P = 0.036), respectively (Fig. 2A). Furthermore, Kaplan-Meier analysis showed a significant survival benefit in the NK012 group compared with the CPT-11 (66.7 mg/kg/d, q4d × 3)/bevacizumab group (P = 0.046) and CPT-11 (40 mg/kg/d, qd × 5)/bevacizumab group (P = 0.0041), respectively (Fig. 2B). However, there was no significant difference between NK012/bevacizumab group and NK012 monotherapy group (P = 0.45; Fig. 2B). There was no severe body weight loss or toxic death according to treatment (Table 1).

Histologic results. Histologic examinations revealed that decreased cellularity, increased tumor stroma, and inflammatory cell infiltration were observed in the tumors treated with NK012. Tumors treated with other regimens showed no apparent morphologic differences from the control tumors (Fig. 3A). Concordant with morphologic changes, the number of Ki-67$^+$ tumor cells decreased in tumors treated with NK012 compared with CPT-11/bevacizumab (Fig. 3A and B; $P < 0.001$). Quantification of VEGF-positive area and microvessel density decreased in tumors treated with NK012 compared with other treatment regimens (Fig. 3A, C, and D; $P < 0.05$). Microvessel density dramatically decreased in tumors treated with bevacizumab in combination with any formulation of the anticancer drug (Fig. 3A and C). The small intestinal mucosa of mice treated

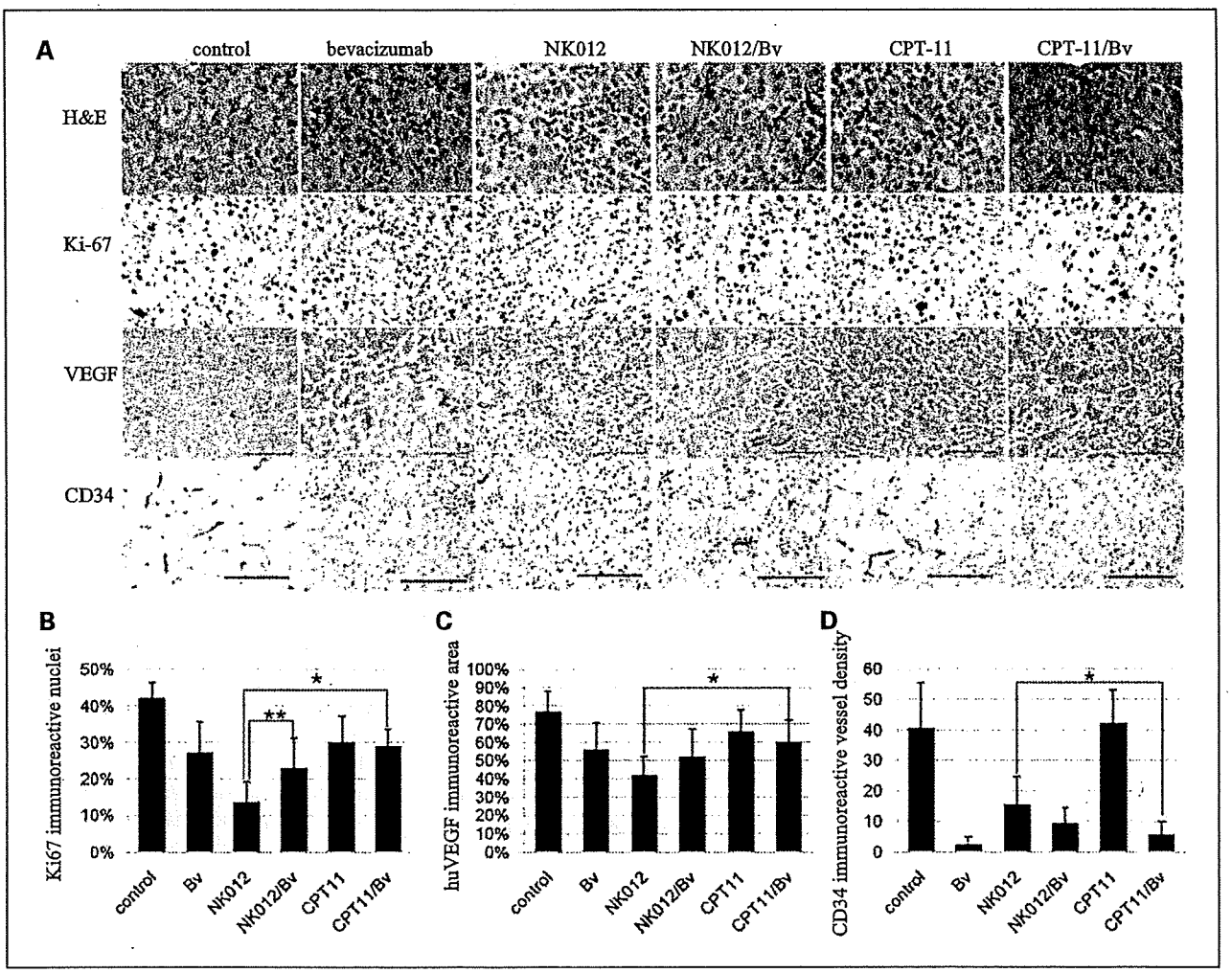

Fig. 3. Tissue-based studies of U87MG/Luc orthotopic xenografts of nude mice treated with NK012, CPT-11, bevacizumab, NK012/bevacizumab, or CPT-11/bevacizumab. *A*, H&E staining of representative xenograft regions (magnification, ×400). Immunohistochemical analysis of tumor cells stained with anti–Ki-67 nuclear antigen, anti-VEGF, and angiogenesis with anti-CD34 antibody (bar, 100 μm). Comparison between xenografts treated with each regimen. *B*, proliferation index by Ki-67. *C*, human VEGF immunoreactive area (%). *D*, angiogenesis by vessel density. *, $P < 0.01$; **, $P < 0.05$ (two-tailed Student's t test).

with NK012 or NK012/bevacizumab showed no histologic changes including fibrosis, active inflammation, or shortening and decrease in number of villi in the small intestinal mucosa as reported previously (ref. 17; data not shown).

Tissue concentration of free SN-38 after administration of NK012 and CPT-11 in combination with bevacizumab. The concentration of free SN-38 in orthotopic glioblastoma tissue after the administration of NK012 and CPT-11 in combination with bevacizumab was examined to evaluate the interaction between these anticancer agents. In the case of NK012 administration in combination with bevacizumab, free SN-38 concentration in tumor tissue was significantly decreased compared with SN-38 concentration when NK012 was administered alone (Fig. 4A; P = 0.027). On the other hand, in the case of CPT-11 administration in combination with bevacizumab, free SN-38 concentration in tumor tissue was almost similar to SN-38 concentration when CPT-11 was administered alone (Fig. 4B; P = 0.66).

Discussion

Concomitant chemoradiotherapy with surgery followed by single-agent adjuvant treatment with the alkylating agent temozolomide is the current standard of care for the patients with glioblastoma multiforme (3). However, tumor recurrence is experienced by almost all glioblastoma multiforme patients after the first-line therapy. Combination therapy of CPT-11 with bevacizumab is now a recognized second-line therapy in recurrent glioblastoma multiforme.

The main purpose of this study was to clarify the advantage of combination therapy of NK012, a SN-38–incorporating polymeric micelle, with bevacizumab against orthotopic U87MG glioblastoma multiforme tumor in mice. Single use of NK012 exerted superior antitumor activity in the orthotopic tumors compared with CPT-11 combined with bevacizumab. The NK012 single-agent treatment group showed the most prolonged survival of all treatment groups, and a statistically significant difference was revealed by the Kaplan-Meier analysis compared with the CPT-11/bevacizumab group (66.7 mg/kg/d, q4d × 3; P = 0.046 and 40 mg/kg/d, qd × 5; P = 0.0041).

The present study showed that the addition of the anti-VEGF monoclonal antibody bevacizumab to the CPT-11 therapy resulted in markedly increased activity, the same as reported clinically (9, 10). Although the mechanisms underlying the activities of bevacizumab remain unclear, the following factors are considered to be important: direct antiangiogenic effects and cytotoxics against vascular endothelial cells and other stromal elements, direct effects on tumor cells expressing VEGF receptors and stem cell–like glioma cells (18), and improvement of the delivery of anticancer drug by forced normalization of tumor vasculature (19). Bevacizumab is a humanized monoclonal antibody that does not cross-react with mouse VEGF, and the efficacy and toxicity in combination with cytotoxic drugs are not the same in mouse and human. In mice, however, bevacizumab can react with VEGF secreted from human tumor xenograft and leads to tumor vessel decrease, reduction in vessel permeability and diameter (20), and decrease in interstitial fluid pressure in xenografts (21).

NK012, a novel SN-38–incorporating polymeric micelle, is a prodrug of SN-38 similar to CPT-11. Although CPT-11 is converted to SN-38 in tumors by carboxylesterase, the metabolic conversion rate is within 2% to 8% of the original volume of CPT-11 (22, 23). In contrast, the release rate of SN-38 from NK012 is 74% under physiologic pH conditions even without carboxylesterases (12). Recently, we showed that NK012 exerted significantly more potent antitumor activity against various human tumor xenografts compared with CPT-11 (12, 24–26). The diameter of a micelle carrier is in the approximate range of 10 to 100 nm. Although this size is small, it is still sufficiently large to prevent renal secretion of the carrier. The micelle system can evade nonspecific capture by the

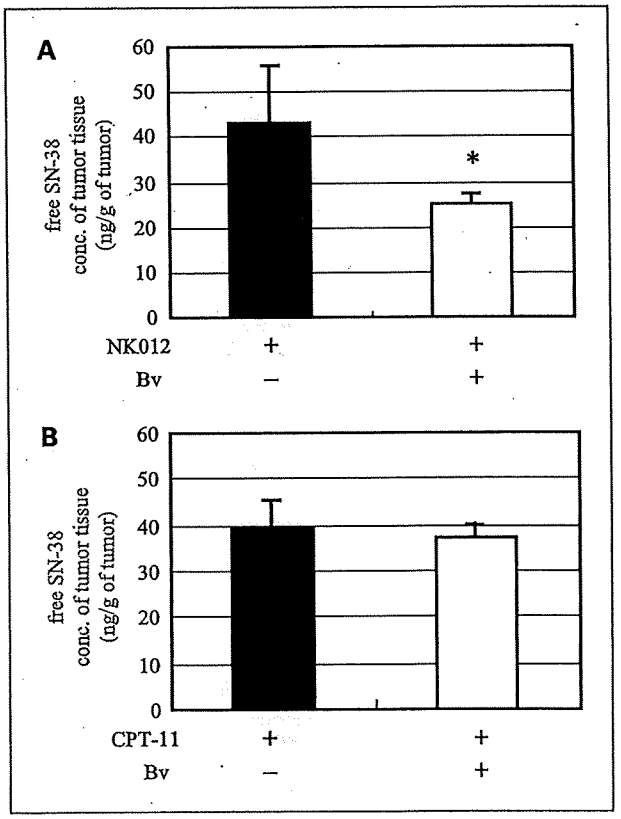

Fig. 4. Concentration of free SN-38 of tumor tissue at T_{max}. NK012 (30 mg/kg intravenously), CPT-11 (66.7 mg/kg intravenously), or bevacizumab (5 mg/kg intraperitoneally) was administered 28 d after intracranial injection of U87MG/Luc (*columns*, mean; *bars*, SD). *A*, concentration (*conc.*) of free SN-38 in glioma tissue of U87MG/Luc mouse model after administration of NK012 alone (*black column*) and NK012 with bevacizumab (*white column*). *B*, concentration of free SN-38 in glioma tissue of U87MG/Luc mouse model after administration of CPT-11 alone (*black column*) and CPT-11 with bevacizumab (*white column*). *, $P < 0.05$, significant to NK012 alone (two-tailed Student's t test).

reticuloendothelial system in various organs because the outer shell of the micelle is covered with polyethylene glycol. Therefore, a drug-incorporating micelle can be expected to have a long plasma half-life, which permits a large amount of the micelles to reach tumor tissues, extravasate from tumor capillaries, and then be retained in tumor tissues for a long time by using the enhanced permeability and retention effect (11). This prolonged retention of NK012 in the tumor and sustained release of free SN-38 from NK012 may be responsible for its more potent antitumor activity observed in the present study (27).

In this study, the antitumor effect was observed by means of bioluminescence imaging. Bioluminescence imaging revealed antitumor activity compared with CPT-11 in combination with bevacizumab. However, antiangiogenic agents can suppress the extravasation of contrast agents such as gadolinium, and gadolinium-contrast magnetic resonance imaging may give a false response (28). This means that bevacizumab is suspected of having a negative effect on bioluminescence imaging by reducing the permeability of tumor vessels. Therefore, we also evaluated the antitumor activity pathologically and immunohistochemically. Consequently, the NK012 group showed a high therapeutic advantage in Ki-67 index in a pathology analysis compared with the other treatment groups.

Interestingly, bevacizumab could not potentiate the antitumor activity of NK012 and elongate the survival of NK012. In the present pharmacologic study, the free SN-38 concentration in the tumor tissue decreased significantly when NK012 was administered in combination with bevacizumab compared with NK012 monotherapy. Results available to date and the results from the present study lead to the consideration that the reduced accumulation of NK012 by bevacizumab may cancel the direct effect of bevacizumab and NK012 against orthotopic glioma in mice. The influence of bevacizumab might be different in macromolecule such as NK012 and small compound such as CPT-11. Enhanced vascular permeability might be more important for macromolecule than small molecule. A further study is necessary to clarify the phenomenon. Dose-limiting toxicities of CPT-11 are neutropenia and diarrhea. Diarrhea was not observed in the NK012 treatment group, and the intestinal toxicity was not observed by the pathology examination as reported previously (17). As for this, it is understood that serious diarrhea has not been reported in MTD of NK012 in two phase I clinical trials against advanced solid tumors in Japan and the United States (29, 30).

In conclusion, NK012 showed a higher therapeutic index in U87MG glioblastoma in mice compared with CPT-11/bevacizumab. Therefore, data from the present study may warrant further preclinical evaluation of NK012 before conducting the clinical trial of the drug.

Disclosure of Potential Conflicts of Interest

No potential conflicts of interest were disclosed.

Acknowledgments

We thank N. Mie and M. Ohtsu for technical assistance and K. Shiina for secretarial assistance.

Grant Support

Grant-in-Aid for Third-Term Comprehensive Control Research for Cancer from the Ministry of Health, Labor and Welfare of Japan; grant 17016087 for Scientific Research on Priority Areas from the Ministry of Education, Culture, Sports, Science and Technology; and Japanese Foundation for Multidisciplinary Treatment of Cancer (Y. Matsumura) and Princess Takamatsu Cancer Research Fund 07-23908.

The costs of publication of this article were defrayed in part by the payment of page charges. This article must therefore be hereby marked *advertisement* in accordance with 18 U.S.C. Section 1734 solely to indicate this fact.

Received 9/2/09; revised 11/2/09; accepted 11/9/09; published OnlineFirst 1/12/10.

References

1. Takano S, Yoshii Y, Kondo S, et al. Concentration of vascular endothelial growth factor in the serum and tumor tissue of brain tumor patients. Cancer Res 1996;56:2185–90.
2. Kleihues P, Louis DN, Scheithauer BW, et al. The WHO classification of tumors of the nervous system. J Neuropathol Exp Neurol 2002;61:215–25, discussion 226–9.
3. Stupp R, Mason WP, van den Bent MJ, et al. Radiotherapy plus concomitant and adjuvant temozolomide for glioblastoma. N Engl J Med 2005;352:987–96.
4. Wong ET, Hess KR, Gleason MJ, et al. Outcomes and prognostic factors in recurrent glioma patients enrolled onto phase II clinical trials. J Clin Oncol 1999;17:2572–8.
5. Friedman HS, Petros WP, Friedman AH, et al. Irinotecan therapy in adults with recurrent or progressive malignant glioma. J Clin Oncol 1999;17:1516–25.
6. Cloughesy TF, Filka E, Kuhn J, et al. Two studies evaluating irinotecan treatment for recurrent malignant glioma using an every-3-week regimen. Cancer 2003;97:2381–6.
7. Chamberlain MC. Salvage chemotherapy with CPT-11 for recurrent glioblastoma multiforme. J Neurooncol 2002;56:183–8.
8. Prados MD, Lamborn K, Yung WK, et al. A phase 2 trial of irinotecan (CPT-11) in patients with recurrent malignant glioma: a North American Brain Tumor Consortium study. Neuro Oncol 2006;8:189–93.
9. Vredenburgh JJ, Desjardins A, Herndon JE 2nd, et al. Phase II trial of bevacizumab and irinotecan in recurrent malignant glioma. Clin Cancer Res 2007;13:1253–9.
10. Vredenburgh JJ, Desjardins A, Herndon JE 2nd, et al. Bevacizumab plus irinotecan in recurrent glioblastoma multiforme. J Clin Oncol 2007;25:4722–9.
11. Matsumura Y, Maeda H. A new concept for macromolecular therapeutics in cancer chemotherapy: mechanism of tumoritropic accumulation of proteins and the antitumor agent smancs. Cancer Res 1986;46:6387–92.
12. Koizumi F, Kitagawa M, Negishi T, et al. Novel SN-38-incorporating polymeric micelles, NK012, eradicate vascular endothelial growth factor-secreting bulky tumors. Cancer Res 2006;66:10048–56.

13. Kuroda J, Kuratsu J, Yasunaga M, Koga Y, Saito Y, Matsumura Y. Potent antitumor effect of SN-38-incorporating polymeric micelle, NK012, against malignant glioma. Int J Cancer 2009;124: 2505–11.
14. Vassal G, Terrier-Lacombe MJ, Bissery MC, et al. Therapeutic activity of CPT-11, a DNA-topoisomerase I inhibitor, against peripheral primitive neuroectodermal tumour and neuroblastoma xenografts. Br J Cancer 1996;74:537–45.
15. Kawato Y, Furuta T, Aonuma M, Yasuoka M, Yokokura T, Matsumoto K. Antitumor activity of a camptothecin derivative, CPT-11, against human tumor xenografts in nude mice. Cancer Chemother Pharmacol 1991;28:192–8.
16. Vassal G, Boland I, Santos A, et al. Potent therapeutic activity of irinotecan (CPT-11) and its schedule dependency in medulloblastoma xenografts in nude mice. Int J Cancer 1997;73:156–63.
17. Nagano T, Yasunaga M, Goto K, et al. Antitumor activity of NK012 combined with cisplatin against small cell lung cancer and intestinal mucosal changes in tumor-bearing mouse after treatment. Clin Cancer Res 2009;15:4348–55.
18. Bao S, Wu Q, Sathornsumetee S, et al. Stem cell-like glioma cells promote tumor angiogenesis through vascular endothelial growth factor. Cancer Res 2006;66:7843–8.
19. Weis SM, Cheresh DA. Pathophysiological consequences of VEGF-induced vascular permeability. Nature 2005;437:497–504.
20. Yuan F, Chen Y, Dellian M, Safabakhsh N, Ferrara N, Jain RK. Time-dependent vascular regression and permeability changes in established human tumor xenografts induced by an anti-vascular endothelial growth factor/vascular permeability factor antibody. Proc Natl Acad Sci U S A 1996;93:14765–70.
21. Lee CG, Heijn M, di Tomaso E, et al. Anti-vascular endothelial growth factor treatment augments tumor radiation response under normoxic or hypoxic conditions. Cancer Res 2000;60:5565–70.
22. Slatter JG, Schaaf LJ, Sams JP, et al. Pharmacokinetics, metabolism, and excretion of irinotecan (CPT-11) following I.V. infusion of [(14)C] CPT-11 in cancer patients. Drug Metab Dispos 2000;28:423–33.
23. Rothenberg ML, Kuhn JG, Burris HA 3rd, et al. Phase I and pharmacokinetic trial of weekly CPT-11. J Clin Oncol 1993;11:2194–204.
24. Sumitomo M, Koizumi F, Asano T, et al. Novel SN-38-incorporated polymeric micelle, NK012, strongly suppresses renal cancer progression. Cancer Res 2008;68:1631–5.
25. Nakajima TE, Yasunaga M, Kano Y, et al. Synergistic antitumor activity of the novel SN-38-incorporating polymeric micelles, NK012, combined with 5-fluorouracil in a mouse model of colorectal cancer, as compared with that of irinotecan plus 5-fluorouracil. Int J Cancer 2008;122:2148–53.
26. Saito Y, Yasunaga M, Kuroda J, Koga Y, Matsumura Y. Enhanced distribution of NK012, a polymeric micelle-encapsulated SN-38, and sustained release of SN-38 within tumors can beat a hypovascular tumor. Cancer Sci 2008;99:1258–64.
27. Kawato Y, Aonuma M, Hirota Y, Kuga H, Sato K. Intracellular roles of SN-38, a metabolite of the camptothecin derivative CPT-11, in the antitumor effect of CPT-11. Cancer Res 1991;51:4187–91.
28. Olivero WC, Dulebohn SC, Lister JR. The use of PET in evaluating patients with primary brain tumours: is it useful? J Neurol Neurosurg Psychiatry 1995;58:250–2.
29. Burris HA 3rd, Infante JR, Spigel DR, et al. A phase I dose-escalation study of NK012. Proc Am Soc Clin Oncol 2008, abstract 2538.
30. Kato K, Hamaguchi T, Shirao K, et al. Interim analysis of phase I study of NK012, polymer micelle SN-38, in patients with advanced cancer. Proc Am Soc Clin Oncol 2008, abstract 485.

EUROPEAN JOURNAL OF CANCER XXX (2009) XXX–XXX

available at www.sciencedirect.com

ScienceDirect

journal homepage: www.ejconline.com

Antitumour activity of NK012, SN-38-incorporating polymeric micelles, in hypovascular orthotopic pancreatic tumour

Yohei Saito [a,b], *Masahiro Yasunaga* [a], *Jun-ichiro Kuroda* [a], *Yoshikatsu Koga* [a], *Yasuhiro Matsumura* [a,*]

[a] *Investigative Treatment Division, Research Center for Innovative Oncology, National Cancer Center Hospital East, 6-5-1 Kashiwanoha, Kashiwa, Chiba 277-8577, Japan*

[b] *Laboratory of Cancer Biology, Department of Integrated Biosciences, Graduate School of Frontier Sciences, The University of Tokyo, 5-1-5 Kashiwanoha, Kashiwa, Chiba 277-8562, Japan*

ARTICLE INFO

Article history:
Received 10 September 2009
Received in revised form 6 November 2009
Accepted 19 November 2009
Available online xxxx

Keywords:
Pancreatic cancer
DDS (drug delivery system)
Polymer micelles
NK012

ABSTRACT

Human pancreatic cancer is refractory to chemotherapy partly because of blockage to penetration of anticancer agents. This issue must be taken into account particularly for the drug delivery system (DDS). The aim of the present study is to investigate how NK012 (SN-38-incorporating polymeric micelles) categorised as DDS exerts its antitumour effect in an orthotopic pancreatic tumour model compared with gemcitabine and irinotecan hydrochloride (CPT-11), a low-molecular-weight prodrug of a 7-ethyl-10-hydroxy-camptothecin (SN-38).

The maximum tolerated doses (MTDs) of NK012 (30 mg/kg/d), CPT-11 (66.7 mg/kg/d) and gemcitabine (16.5 mg/kg/d) were administered to mice bearing human pancreatic cancer cell (SUIT-2) xenografts implanted orthotopically. Antitumour effects of these compounds were evaluated. Drug distribution within the tumour was examined by fluorescence microscopy and high performance liquid chromatography (HPLC).

NK012 exerted potent antitumour effects compared with CPT-11 and gemcitabine. A high concentration of NK012 and SN-38 released from NK012 had been observed until 192 h. On the other hand, SN-38 converted from CPT-11 was detected only 1 h postinjection. Fluorescence from NK012 was detected up to 48 h, whereas that from CPT-11 almost disappeared by 24 h postinjection.

NK012 appeared to exert potent antitumour activity against intractable stroma-rich orthotopic pancreatic tumour xenografts due to its sufficient accumulation followed by the effective sustained release of SN-38 from NK012.

1. Introduction

Human pancreatic cancer is well known to have the worst prognosis.[1] At the time of diagnosis, the vast majority of the cancer extends beyond the pancreas. Direct invasion to nearby organs such as the stomach, duodenum, colon, spleen and kidney is common. Distant metastasis to the liver and peritoneal dissemination are also common.[2,3] Gemcitabine is a first-line therapy for patients with advanced pancreatic cancer; however, only a response rate within 6–11% was observed in pancreatic cancer patients treated with gemcitabine.[4,5] The recent success of molecular-targeting agents has some

* *Corresponding author*: Tel./fax: +81 4 7134 6857.
E-mail address: yhmatsum@east.ncc.go.jp (Y. Matsumura).

0959-8049/$ - see front matter © 2009 Elsevier Ltd. All rights reserved.
doi:10.1016/j.ejca.2009.11.014

impact on pancreatic cancer treatment. A recent phase III trial of gemcitabine alone versus gemcitabine and erlotinib (a tyrosine kinase inhibitor) in patients with advanced pancreatic cancer showed that overall survival was significantly improved with gemcitabine and erlotinib than with gemcitabine and placebo. However, the improvement in median overall survival with gemcitabine and erlotinib was modest (6.24 months versus 5.91 months).[6] Therefore, novel therapeutic approaches against invasive advanced pancreatic cancer are urgently needed.

There are several reasons why pancreatic cancer is intractable clinically. One is that anticancer drugs are not efficiently and sufficiently delivered to the cancer cells within pancreatic cancer tissues. This is because human pancreatic cancer is hypovascular[7,8] and is rich in interstitial tissue, which may hinder the efficient distribution of anticancer drugs to the entire pancreatic cancer tissue.

Passive targeting by the drug delivery system is based on the pathological features of many kinds of solid tumours. Solid tumours generally have the features of hypervascularity, irregular vascular architecture, enhanced vascular permeability and the absence of an effective lymphatic drainage that prevents efficient clearance of macromolecules. Using these characteristic tumour vasculatures, macro-molecular agents accumulate selectively in solid tumours compared with low-molecular agents, with less distribution to normal tissues. These vascular characteristics of solid tumours are the basis of the enhanced permeability and retention (EPR) effect.[9]

SN-38, a biologically active metabolite of CPT-11 has potent antitumour activity against several cancers.[10,11] However, it has not yet been used clinically because of its water insolubility and severe toxicity.[12,13] It has been recently shown that NK012, SN-38-incorporating polymeric micelles, can accumulate selectively in solid tumours by utilising the EPR effect and exerts significantly more potent activity against various human tumour xenografts than CPT-11.[14–18] In pancreatic cancer, we found that NK012 but not CPT-11 could eradicate subcutaneous pancreatic tumour xenografts[19] because of enhanced accumulation, distribution and retention within tumour tissues and the sustained release of SN-38 from NK012.

In the present study, we examined the antitumour effects and pharmaceutical features of NK012 compared with those of CPT-11 and gemcitabine using orthotopic human pancreatic cancer xenografts that are more similar to human pancreatic cancers in terms of tumour vascularity and interstitium.

2. Materials and methods

2.1. Drugs and cells

NK012 was prepared and supplied by Nippon Kayaku Co., Ltd. (Tokyo, Japan). CPT-11 was purchased from Yakult Co., Ltd. (Tokyo, Japan). SN-38 was supplied by Yakult Co., Ltd. Gemcitabine was purchased from Eli Lilly Japan K.K. (Kobe, Japan). The human pancreatic cancer cell line SUIT-2 was purchased from the Health Science Research Resources Bank (Osaka, Japan). SUIT-2 cells were maintained in Dulbecco's modified Eagle's medium supplemented with 10% foetal bovine serum (Cell Culture Technologies, Gaggenau-Hoerden, Germany), 100 units/ml streptomycin and 2 mmol/L L-glutamine (Sigma, St. Louis, MO, United States of America) in an atmosphere of 5% CO_2 at 37 °C.

2.2. Orthotopic pancreatic cancer mouse model

Four-weeks-old female BALB/c nude mice were purchased from CLEA Japan (Tokyo, Japan). SUIT-2 cells (5×10^6) were injected into the body of the pancreas of nude mouse after laparotomy under anaesthesia. All animal procedures were performed in compliance with the Guideline for the Care and Use of Experimental Animals established by the Committee for Animal Experimentation of the National Cancer Center, Japan; these guidelines meet the ethical standards required by law for the use of experimental animals in Japan.

2.3. In vitro growth inhibition assay

Cell toxicity of NK012, SN-38, CPT-11 and gemcitabine was measured by tetrazolium salt-based proliferation assay (WST-8 assay; Wako Chemicals, Osaka, Japan), as described previously.[19] Data were averaged and normalised against a non-treated control to generate dose–response curves. The number of living cells (% Control) was calculated using the following formula: % Control = (Each absorbance – Absorbance of blank well)/Absorbance of control well × 100.

2.4. Establishment of SUIT-2 cell lines stably expressing firefly luciferase and YFP mutant Venus

For the *in vivo* bioluminescence imaging of orthotopic pancreatic tumours, the SUIT-2 cell line stably expressing firefly luciferase and the yellow fluorescent protein (YFP) mutant Venus were established. The coding sequence for firefly luciferase and Venus was subcloned into the pIRES Vector (Clontech Laboratories, Mountain View, CA, United States of America). The fragment consists of Luciferase-IRES-Venus generated from the plasmid with the restriction enzymes Nhe I and Not I. This fragment was subcloned into the pEF6/V5-His Vector (Invitrogen, Carlsbad, CA, United States of America) to generate plasmids of pEF6-Luciferase-IRES-Venus. SUIT-2 cells were transfected with these plasmids. Thereafter, we established SUIT-2 cell lines stably expressing firefly luciferase and the YFP mutant Venus.

2.5. Histological and immunohistochemical analyses

Tumour tissues were fixed in 10% formalin, and paraffin sections were prepared by the Tokyo Histopathologic Laboratory Co., Ltd. (Tokyo, Japan). For blood vessel staining, the sections were soaked 3 times for 5 min each in xylene, and then 3 times for 3 min each in ethanol to remove the paraffin. The sections were then rinsed with phosphate buffered saline (PBS), and endogeneous peroxidase was blocked with a 0.3% hydrogen peroxide solution in 100% methanol for 20 min, followed by 3 times of PBS rinses for 5 min. Then, Proteinase K (Dako, Glostrup, Denmark) was added. After the sections were rinsed 3 times for 5 min each with PBS, non-specific protein binding was blocked with 5% skim milk (BD, Franklin Lakes, NJ, United States of America) in PBS for 30 min at room

Please cite this article in press as: Saito Y. et al., Antitumour activity of NK012, SN-38-incorporating polymeric micelles, in hypovascular orthotopic pancreatic tumour, *Eur. J. Cancer* (2009), doi:10.1016/j.ejca.2009.11.014